View metadata, citation and similar papers at core.ac.uk
brought to you by CORE
provided by OTHES

universität
wien

DIPLOMARBEIT

Titel der Diplomarbeit

A non-commutative QFT at the self-dual point

angestrebter akademischer Grad

Magister der Naturwissenschaften (Mag. rer. nat.)

Verfasser:	Thomas Kaltenbrunner
Matrikel-Nummer:	0301246
Studienrichtung:	411 Physik
Betreuer:	Ao. Univ.-Prof. Dr. Harald Grosse

Wien, am 25. März 2009

Danksagung

Ich möchte meinem Betreuer, Professor Harald Grosse herzlich für die hilfreichen Diskussionen und Hinweise bei aufgetretenen Fragen während des letzten Jahres danken und dafür, dass er mich auf dieses interessante Thema hingewiesen hat. Weiters bedanke ich mich bei meiner Familie die mir erst die Möglichkeit gegeben hat Physik zu studieren. Ich danke auch Georg und Anas für die vielen interessanten Diskussionen in denen ich das Thema von verschiedensten Seiten beleuchten konnte.

Ganz besonders bedanke ich mich bei meiner Freundin Irmi für die Unterstützung und aufmunternden Gespräche die mir geholfen haben meine Begeisterung auch in schwierigen Zeiten beizubehalten.

Abstract

In this tesis the Grosse-Wulkenhaar-model at the self-dual point $\Omega = 1$ is examined. The relevant 2-point and 4-point Feynman graphs are renormalized up to two loop order to proof the boundedness of the β-function by showing that the difference between bare and renormalized coupling constant is finite. This result is then generalized up to all orders by using Ward-Identites and the Dyson-Schwinger-Equation. Additionally the relations between (2n-2)- and 2n-point functions, obtained through the Ward-Identities, are calculated explicitly between 2 and 4-point functions. The last section uses the techniques of the general proof to show the boundedness of the β-function of the Grosse-Wulkenhaar-model in a magnetic field, namely the Langmann-Szabo-Zarembo model with oscillator term, which is an interesting toy model of the Quantum Hall Effect.

Contents

1 Introduction **1**

2 Definitions and Theorem **3**

3 Renormalization in 2D **5**

3.1 First-order-renormalization 6

3.2 Two-loop-Renormalization 7

4 Renormalization in 4 Dimensions **11**

4.1 Renormalization of 2-point-graphs at 1-loop-level 11

4.1.1 Mass-renormalization 12

4.1.2 Calculation of the prefactor 12

4.1.3 Field-strength-renormalization 13

4.2 Two-loop-calculation 13

4.2.1 Asymptotical behaviour of the divergent graphs 14

4.2.2 Mass-renormalization 14

4.2.3 Field-strength-renormalization 17

4.3 4-pt-function 17

5 Boundedness of β-function **21**

5.1 First-order-contribution 22

5.2 Second-order-contribution 22

6 Vanishing Of Beta-Function Up To All Orders **25**

6.1 The Ward Identities 25

6.2 Proof of the Theorem 27

6.2.1 Graph $G^4_{(1)}$ 28

6.2.2 Graph $G^4_{(3)}$ 30

6.2.3 Result 33

7 Explicit Calculation of Ward Identities **35**

7.1 One-loop-calculation 35

7.2 Two-loop-calculation 36

7.2.1 Ward Identity corresponding to the TEXTup graph 36

7.2.2 Ward Identity corresponding to the TINTup graph 37

7.2.3 Ward Identity corresponding to the S graph 38

8 Grosse-Wulkenhaar-model in a magnetic field 41
- 8.1 Ward Identities 42
- 8.2 Proofing the theorem 43

9 Final Remarks 47

10 Appendix 49
- 10.1 Two-Loop-Calculation 49
  - 10.1.1 TEXTup 50
  - 10.1.2 TINTup 51
  - 10.1.3 TINTdown and TEXTdown 53
  - 10.1.4 S 53

11 Zusammenfassung 55

Chapter 1

Introduction

The best studied non-commutative space in QFT is certainly the Moyal space. It is defined as the algebra $\mathbb{R}^D_\theta$ whose elements fulfill the relation

$$[x_i, x_j] = i\Theta_{ij} \tag{1.1}$$

with Θ being a non-degenerate, skew-symmetric matrix. For the easiest and most common Moyal space one writes Θ as

$$\Theta = \begin{pmatrix} 0 & \theta_1 & & (0) & \\ -\theta_1 & 0 & & & \\ & & \ddots & & \\ & (0) & & 0 & \theta_{D/2} \\ & & & -\theta_{D/2} & 0 \end{pmatrix} \tag{1.2}$$

and sets all components θ constant and equal to each other. As a vector space, this algebra is now given by $S(\mathbb{R}^4)$ of smooth and rapidly decaying Schwartz-class functions. Those functions are equipped with the multiplication rule

$$(f \star g)(x) = \int \frac{\mathrm{d}^D k}{(2\pi)^D} \int \mathrm{d}^D y f(x + \frac{1}{2}\Theta \cdot k) g(x+y) e^{ik\cdot y} \tag{1.3}$$

All calculations in this tesis are based on this type of Moyal space.

The model I will study is the Grosse-Wulkenhaar-Model, which is an extension of the standard, non-commutative $\phi^{\star 4}$ model

$$S[\phi] = \int \mathrm{d}^4 x \Big\{ \frac{1}{2}(\partial_\mu \phi) \star (\partial^\mu \phi) + \frac{m^2}{2}(\phi \star \phi) + \frac{\lambda}{2} \phi \star \phi \star \phi \star \phi) \Big\} \tag{1.4}$$

where "m" stands for the mass and "λ" for the coupling constant. It has the usual, commutative Lagrangian where the multiplication is replaced by the Moyal star product. Unfortunately this standard $\phi^{\star 4}$ model was found not to be renormalizable because of a new phenomena, the so-called UV-IR mixing discovered by Minwalla, Van Raamsdonk and Seiberg in [1]. This phenomena exhibits a relation between short and long distances, and therefore between the UV- and IR-regime. It is not present in commutative theories and lead to a new type of diverging Feynman graphs which are non-local and therefore cannot be put into a redefinition of the mass. The old hope of an inherent regularization of QFT by using noncommutative space-time structure was thus not fulfilled.

A duality of this model was the first step of the solution to the problem. Langman and Szabo found a symmetry on the Moyal plane between space and momenta in [2]. It states that the interaction part of the standard $\phi^{\star,4}$-model, by substituting

$$\begin{aligned} \hat{\phi}(p) &\longleftrightarrow \pi^2\sqrt{|\det\theta\,|}\phi(x) \qquad p_\mu \longleftrightarrow \tilde{x}_\mu := 2(\theta^{-1})_{\mu\nu}x^\nu \\ \hat{\phi}(p) &= \int \mathrm{d}^4x e^{(-1)^a i p_{a,\mu} x^\mu_a}, \end{aligned} \tag{1.5}$$

where the index “a” refers to the cyclic order of the $\star$-product, has the same form in coordinate and momentum space. This relation was thus not fulfilled for the free part of the Hamiltonian.

Grosse and Wulkenhaar solved the problem of renormalizability by making the free part of the Hamiltonian of the $\phi^{\star 4}$ model invariant under this duality too by adding a harmonic potential term to it with ”Ω“ being the oscillator frequency.

$$S[\phi] = \int \mathrm{d}^4x \Big\{ \frac{1}{2}(\partial_\mu\phi)\star(\partial^\mu\phi) + \frac{\Omega^2}{2}(\tilde{x}_\mu\phi)\star(\tilde{x}^\mu\phi) + \frac{m^2}{2}(\phi\star\phi) + \frac{\lambda}{2}\phi\star\phi\star\phi\star\phi) \Big\} \tag{1.6}$$

The duality is especially obvious by taking a look at the parameters of the theory. Under the above given transformation they change like

$$S[\phi,\mu_0,\lambda,\Omega] \longrightarrow \Omega^2 S[\phi,\frac{\mu_0}{\Omega},\frac{\lambda}{\Omega},\frac{1}{\Omega}] \tag{1.7}$$

By taking the limit $\Omega \to 1$ the dependency of the parameters stays invariant and thus one cannot distinguish anymore between space and momenta. This special value $\Omega = 1$ is called the self-dual point. With this extra term they were now able to show renormalizability of this model in the matrix base first in 2 dimensions and finally in 4D as well [3–5].

Calculating in the matrix base means that the Moyal $\star$-product becomes a simple matrix product, while the fields are then represented as (infinite) matrices. The Feynman graphs then become so-called Ribbon graphs. The single lines of a standard graph are extended to double lines and each single line carries one or more (depending on dimension) indices. If the index values are conserved along a ribbon, i.e. $G_{mn;kl} = G(m,n)\delta_{ml}\delta_{nk}$, where “$G_{mn;kl}$” is the propagator of the model, one speaks of a *local* matrix theory, while otherwise it would be a non-local one. Comparing with the definition of the propagator in the next section (2.1), it can be seen that the GW model at the self-dual point corresponds to a local theory.

The idea of adding an extra term to the Lagrangian of the model to make it renormalizable was used by others to find different renormalizable models, such as the $\phi_2^{\star 3}$-model [6] or the Gross-Neveu-model [7], but still, the GW-model is unique because of a special feature, namely the boundedness of the beta function up to all orders.

The β-function was again first calculated by Grosse and Wulkenhaar in [8] up to one loop order. There they made the amazing discovery that the RG group flow does not show a Landau ghost and is just bounded in the UV-regime! The running coupling constant stays finite, contrary to the classical ϕ^4-theory. Additionally the oscillator paramater Ω tends to one and therefore the self-dual point is a fixed point in the theory. When letting Ω_{ren} tend to zero the oscillator term vanishes and the Landau ghost reappears.

This result was first extended up to three loops by Disertori and Rivasseau in [9] and finally generalized to all loop orders by Disertori, Rivasseau, Gurau and Magnen in [10].

Chapter 2

Definitions and Theorem

The propagator of the GW-model (1.6) in the matrix base at the self-dual point $\Omega = 1$ is given by:

$$C_{mn;kl} = \frac{1}{(4\pi)^2\theta} G_{mn} \delta_{ml} \delta_{nk} \qquad G_{mn} = \frac{1}{A+m+n} \tag{2.1}$$

Here, $A = 2 + \mu^2\theta/4$, where μ is the mass, and the indices m and n are in 4 dimensions $\in \mathbb{N}^2$. This means they are abbreviations for

$$m + n = m_1 + m_2 + n_1 + n_2 \qquad \text{and} \qquad \delta_{ml} = \delta_{m_1 l_1} \delta_{m_2 l_2} \tag{2.2}$$

respectively.

The model can be defined as a complex or a real one.

$$S_r = \frac{(4\pi)^2\theta}{2} \sum_{m,n \in \mathbb{N}^2} \phi_{mn} G^{-1}_{mn} \phi_{mn} + \frac{\lambda}{4}(4\pi^2\theta^2) \sum_{m,n,k,l \in \mathbb{N}^2} \phi_{mn}\phi_{nk}\phi_{kl}\phi_{lm} \tag{2.3}$$

$$S_c = (4\pi)^2\theta \sum_{m,n \in \mathbb{N}^2} \bar{\phi}_{mn} G^{-1}_{mn} \phi_{mn} + \frac{\lambda}{2}(4\pi^2\theta^2) \sum_{m,n,k,l \in \mathbb{N}^2} \bar{\phi}_{mn}\phi_{nk}\bar{\phi}_{kl}\phi_{lm} \tag{2.4}$$

They differ by the orientation of the propagators but when calculating the amplitudes of the diverging graphs, the only differences are numerical factors coming from different orientation of the propagators and the multiplicity of the graphs emerging in the correlation function when contracting the fields. Those differences don't change the behaviour of the diverging graphs and thus one can easily transfer the results obtained in one model to the other. In fact it was shown in [9] that those numerical factors in the two models finally give the same prefactors of the graphs in both of them. The explicit calculation of the renormalized graphs will be done using the real model while the general proof will be based on the complex one.

To show the finiteness of the beta-function one has to compute the evolution equation for the coupling constant

$$\lambda_r = -\frac{1}{4\pi^2\theta^2} \frac{\Gamma_4(0,0,0,0)}{Z^2} \tag{2.5}$$

Here "Z" is the wave function normalization given by

$$Z = 1 - \frac{1}{(4\pi)^2\theta} \partial_{m_1} \Sigma(m,n)\Big|_{m=n=0}. \tag{2.6}$$

The self-energy $\Sigma(m,n)$ is defined as the expectation value of the one-particle-irreducible

Feynman graphs:

$$\Sigma(m,n) =< \phi_{mn}\phi_{nm} >_{1PI} \tag{2.7}$$

Furthermore

$$\Gamma_4(m,n,k,l) =< \phi_{mn}\phi_{nk}\phi_{kl}\phi_{lm} >_{1PI} \ . \tag{2.8}$$

is the amputated 4-point, one-particle-irreducible Green's function.

To do the actual calculation of the evolution equation up to 2-loop-order for λ_r, it is being expanded in the bare coupling constant.

$$\lambda_r = -\frac{1}{4\pi^2\theta^2}\frac{\Gamma_4(0,0,0,0)}{Z^2} = 1 - \gamma_1\tilde{\lambda} + \gamma_2(\tilde{\lambda})^2 + O(\lambda^3) \tag{2.9}$$

where the abbreviation $\tilde{\lambda} = \lambda/16\pi^2$ is defined for convenience.
This proposition has been generalized up to all orders in [10] (see section 6) and states that the equation

Boundedness of β-function 1

$$\Gamma_4(0,0,0,0) = \lambda[1 - \partial_L\Sigma(0,0)]^2 \tag{2.10}$$

holds up to all loop-orders either for

- *the bare equation with fixed ultraviolet cut-off or*
- *the renormalized equation. In that case the coupling constant is still the bare one, but reexpressed as a series in the renormalized one.*

Chapter 3

Renormalization in 2D

To prepare for the more complicated case of Renormalization of the Feynman graphs in 4 dimensions, they are first worked out in 2D.

The only relevant graphs, as shown by Grosse and Wulkenhaar [3], must be planar and have only one external face, which simplifies the calculation a lot. Throughout the calculation I will use the BPHZ renormalization scheme with the renormalization point set to zero, following [9]. The renormalization conditions are

$$\begin{aligned} \Sigma(m,n)\Big|_{m=n=0} &= 0 \\ \frac{\partial\Sigma(m,n)}{\partial m}\Big|_{m=n=0} &= 0 \end{aligned} \tag{3.1}$$

where $\Sigma(m,n)$ stands for the self-energy and instead of m any other external index can be used. Further, the Feynman rules give

- a factor of $\frac{1}{(4\pi)^2\theta}$ for each line
- a contribution of $4\pi^2\theta^2\frac{\lambda}{4}$ for each vertex in the real case.

In 2 dimensions, every index is $\in \mathbb{N}$ and not as in 4 dimensions $\in \mathbb{N}^2$. This means that every index in the Feynman diagrams consists of just one term and not two, as well as the delta functions.

Renormalizing in 2 dimensions one has to deal with less divergences than in four dimensions as there are just logarithmic ones, which are independent of the external momentum. Thus only mass counterterms have to be added. This can be easily verified by checking the degree of divergence:

$$\text{degree of divergence} = \text{dimension of integral} - \text{power of denominator} \tag{3.2}$$

If it is positiv, the integral will converge. If the degree of divergence is smaller or equal zero the term diverges, being logarithmic divergent for zero. Thus, here the only case where an integral can diverge is of the form

$$\int_0^\Lambda \mathrm{d}p \frac{1}{A+p} \tag{3.3}$$

which diverges logarithmically.

3.1 First-order-renormalization

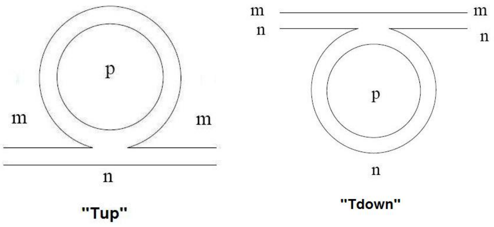

Figure 3.1: 1-loop-graphs: T_{up} and T_{down}

The only graph at first order contributing to the 2-point Green's function is the tadpole graph (see figure 3.1). In matrix theories one usually uses external (or broken) and internal "faces" to calculate the Feynman diagrams instead of using the internal and external momenta like in commutative QFT. Taking the example of the Tadpole, we find one internal face and one external broken face (The number of external faces is bound by the power counting theorem of Grosse and Wulkenhaar to be equal to 1 for relevant graphs). The amplitude of this graph is found by looking at the border of the loop, namely the Ribbon, and adding the corresponding internal and external index plus the mass term to the denominator. The power of the denominator depends on the number of vertices, like in commutative QFT. Therefore, the amplitude of the tadpole is found to be $\frac{1}{A+p+m}$.

Its loop can point either to the upper, or the lower index side. As only the external index is changed, the calculation of the amplitude is the same in both cases.

To find the diverging terms, the following integral for the T_{up}-graph has to be computed:

$$G_{mn}^{T_{up}} = \int\limits_0^\Lambda \mathrm{d}p \frac{1}{A+p+m} = \ln[\Lambda] - \ln[A+m] \tag{3.4}$$

It exhibits a logarithmic divergence which is regularized by the integral where the loop with index p diverges and thus the external index can be neglected.

$$\int\limits_0^\Lambda \mathrm{d}p \frac{1}{A+p} = \ln[\Lambda] - \ln[A] \tag{3.5}$$

This gives the renormalized amplitude for the T_{up} graph:

$$G_{mn}^{T_{up},R} = \ln[\Lambda] - \ln[A+m] - \ln[\Lambda] + \ln[A] = \ln[A] - \ln[A+m] \tag{3.6}$$

Together with the T_{down}-contribution this is the first order term of the self-energy which has to fulfill the renormalization condition (3.1). Obviously, the T_{up} contribution is equal to zero for vanishing external momenta and, as the T_{down} contribution is equal up to exchanging the index m for n, the condition is fullfilled. Thus, we can write down the self-energy up to first order as

$$\frac{1}{(4\pi)^2\theta}\Sigma(m,n) = -\tilde{\lambda}A_{mn} = \frac{\tilde{\lambda}}{4}(2\ln[A] - \ln[A+m] - \ln[A+n]) \tag{3.7}$$

The prefactor 1/4 results from taking into account the combinatorial factors of the graph together with the prefactors coming from the definition of the coupling constant and propagator. The exact calculation is given in the next chapter when renormalizing in 4 dimensions.

3.2 Two-loop-Renormalization

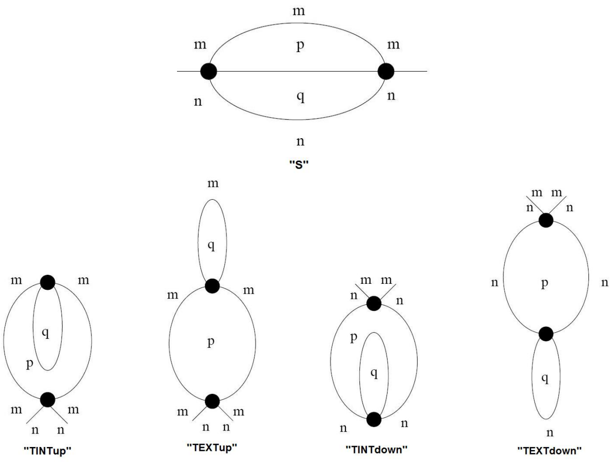

Figure 3.2: 2-loop-diagrams

At the second order there are three different graphs which need renormalization and are shown in figure 3.2.

Starting with the easiest of the three, namely "$TEXT_{up}$", the amplitude is given by

$$
\begin{aligned}
G^{TEXT_{up}} &= \int\limits_0^\Lambda\!\!\int\limits_0^\Lambda \mathrm{d}p\mathrm{d}q \frac{1}{(A+p+m)^2(A+q+m)} = \\
&= \int\limits_0^\Lambda \mathrm{d}p \frac{\ln[\Lambda]-\ln[A+m]}{(A+p+m)^2} = \frac{\ln[\Lambda]}{A+m} - \frac{\ln[A+m]}{A+m}
\end{aligned}
\tag{3.8}
$$

This graph has a subdivergence which has to be renormalized in addition to the overall divergence. Since the two loops p and q don't have any border in common, the overall counterterm, canceling the divergences in the bare graph, and the graph with diverging loop q, is zero. This indicates that the only divergence is the one related to the tadpole graph, which has already been calculated in the last subsection. Together we find the renormalized amplitude as

$$
\begin{aligned}
G_{mn}^{TEXT_{up},R} &= \int\limits_0^\Lambda\!\!\int\limits_0^\Lambda \mathrm{d}p\mathrm{d}q \Big(\frac{1}{(A+p+m)^2(A+q+m)} - \\
&- \frac{1}{(A+p+m)^2(A+q)} - \frac{1}{(A+p)^2(A+q)} + \frac{1}{(A+p)^2(A+q)} \Big) = \\
&= \frac{\ln[A]-\ln[A+m]}{A+m}
\end{aligned}
\tag{3.9}
$$

The amplitude for the graph $TINT_{up}$ is the following:

$$G_{mn}^{TINT_{up}} = \int_0^\Lambda\!\!\int_0^\Lambda \mathrm{d}p\mathrm{d}q \frac{1}{(A+p+m)^2(A+p+q)} =$$
$$= \int_0^\Lambda \mathrm{d}p \frac{\ln[\Lambda]-\ln[A+p]}{(A+p+m)^2} = \frac{\ln[\Lambda]}{A+m} - \frac{\ln[A]}{A+m} - \frac{\ln[A+m]-\ln[A]}{m} \tag{3.10}$$

This graph has a subdivergence too but this time, the corresponding overall counterterm does not cancel. Anyway, the only diverging term is again connected to the tadpole. The overall counterterm gives just finite contributions to fulfill the renormalization condition. Thus,

$$G_{mn}^{TINT_{up},R} = \int_0^\Lambda\!\!\int_0^\Lambda \mathrm{d}p\mathrm{d}q \Big(\frac{1}{(A+p+m)^2(A+p+q)} - \frac{1}{(A+p+m)^2(A+q)} -$$
$$- \frac{1}{(A+p)^2(A+p+q)} + \frac{1}{(A+p)^2(A+q)}\Big) =$$
$$= -\frac{\ln[A+m]-\ln[A]}{m} + \frac{1}{A} \tag{3.11}$$

which goes to zero for $m \to 0$.

The last graph at two loop order is the sunrise graph with the corresponding amplitude given by:

$$G_{mn}^{S} = \int_0^\Lambda\!\!\int_0^\Lambda \mathrm{d}p\mathrm{d}q \frac{1}{(A+p+m)(A+p+q)(A+q+n)} =$$
$$= \frac{1}{(A+m+n)}\Big\{\frac{\pi^2}{6} + \frac{\ln[A+m]^2}{2} - \ln[A]\ln[n] + \ln[A]\ln[A+n] -$$
$$- \ln[A+m]\ln[A+n] + \ln[n]\ln[A+n] - \frac{\ln[A+n]^2}{2} + Li_2[\frac{m}{A+m}]\Big\} \tag{3.12}$$

Already by checking the degree of divergence it can be seen that this graph shows no divergences in 2 dimensions. By adding the order of the integral over p and q we have a dimension of 2 and the power of the denominator is 3. Therefore, no overall divergence is expected. Further the seperated integrals, which have dimension 1, and the power of the denominator for seperate p and q, which are both 2, show that there is no subdivergence neither. Nevertheless, to fulfill the renormalization condition of a vanishing self energy at $m = n = 0$ we have to renormalize the graphs by a finite counterterm.

$$G_{mn}^{S,R} = \int_0^\Lambda\!\!\int_0^\Lambda \mathrm{d}p\mathrm{d}q \Big\{\frac{1}{(A+p+m)(A+p+q)(A+q+n)} -$$
$$- \frac{1}{(A+p)(A+p+q)(A+q)}\Big\} \tag{3.13}$$

In four dimensions, subdivergences will arise and therefore more counterterms will be needed but in 2 dimensions, as we only want to cancel finite terms in our bare graph, just the overall counterterm needs to be subtracted. This gives the final result for the amplitude of the graph:

$$G^{S,R}_{mn} = \frac{1}{A+m+n}\Big\{\frac{\pi^2}{6} + \frac{\ln[A+m]^2}{2} - \ln[A]\ln[n] + \ln[A]\ln[A+n] - \\ - \ln[A+m]\ln[A+n] + \ln[n]\ln[A+n] - \frac{\ln[A+n]^2}{2} + Li_2[\frac{m}{A+m}]\Big\} - \frac{\pi^2}{6A} \tag{3.14}$$

Therefore, the self-energy is up to 2-loop-order in 2 dimensions given by

$$\begin{aligned} \frac{1}{(4\pi)^2\theta}\Sigma(m,n) &= -\tilde{\lambda}A_{mn} + \tilde{\lambda}^2 B^2_{mn} = \\ &= \tilde{\lambda}(2\ln[A] - \ln[A+m] - \ln[A+n]) + \\ &+ \tilde{\lambda}^2\Big(\frac{\ln[A] - \ln[A+m]}{A+m} + \frac{\ln[A] - \ln[A+n]}{A+n} + \\ &+ \frac{\ln[A+m] - \ln[A]}{m} + \frac{\ln[A+n] - \ln[A]}{n} + \frac{2}{A} + \\ &+ \frac{\pi^2}{6(A+m+n)} + \frac{\ln[A+m]^2}{2(A+m+n)} - \frac{\ln[A]\ln[n]}{A+m+n} + \\ &+ \frac{\ln[A]\ln[A+n]}{A+m+n} - \frac{\ln[A+m]\ln[A+n]}{A+m+n} + \frac{\ln[n]\ln[A+n]}{A+m+n} - \\ &- \frac{\ln[A+n]^2}{2(A+m+n)} + \frac{Li_2[\frac{m}{A+m}]}{A+m+n} - \frac{\pi^2}{6A}\Big) \end{aligned} \tag{3.15}$$

Chapter 4

Renormalization in 4 Dimensions

Before we show the boundedness of the beta-function of the GW-model up to all orders in section 6 on page 25, we want to carry out the calculation explicitly up to two-loop-order in 4 dimensions. To do this, we first have to renormalize the relevant 2- and 4-point-graphs. The Feynman rules and the Renormalization scheme stay the same as in 2 dimensions. A detailed introduction to non-commutative Renormalization can be found in [11].

4.1 Renormalization of 2-point-graphs at 1-loop-level

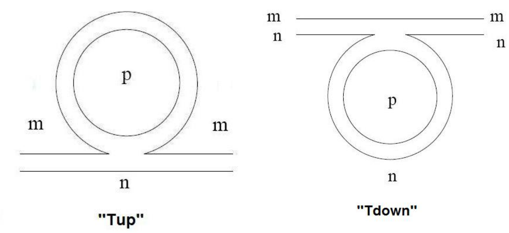

Figure 4.1: 1-loop-graphs: T_{up} and T_{down}

The only one-loop-graph we have to take into account is the Tadpole (see figure 4.1), which can have its loop on the upper or lower index side. In commutative QFT it would be zero but this changes in the noncommutative frame. The amplitude of this graph is given by:

$$G_{mn}^{T_{up}} = \int_0^\Lambda\!\!\int_0^\Lambda \frac{\mathrm{d}^2 p}{(A+p+m)} \qquad G_{mn}^{T_{down}} = \int_0^\Lambda\!\!\int_0^\Lambda \frac{\mathrm{d}^2 p}{(A+p+n)} \tag{4.1}$$

The asymptotic behavior for the diverging loop is:

$$G_{mn}^{T_{up}} \overset{\Lambda\to\infty}{=} 2\ln[2]\Lambda - (A+m)\ln[\Lambda] \tag{4.2}$$

This graph is quadratically divergent in 4 dimensions which is interpreted as a mass divergence, given by the graph with both loops going to infinity, which we have to subtract. As can be seen in Equation (4.2) this graph has a logarithmic divergence which depends on the external momentum as well. Therefore, we will need to add a field-strength renormalization also.

4.1.1 Mass-renormalization

The counterterm is given as the amplitude for the graph, where the loop p diverges. This means the external momentum m can be neglected. Graphically this is depicted in figure 4.2.

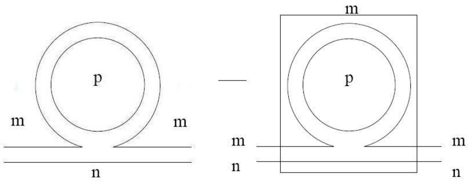

Figure 4.2: T_{up} - mass CT

The renormalized amplitude can now be written down:

$$G_{mn}^{T_{up},R} = \int_0^\Lambda \mathrm{d}^2 p \Big(\frac{1}{(A+p+m)} - \frac{1}{(A+p)} \Big) = \\ = -\, m \ln[\Lambda] + m \ln[2] + (A+m) \ln[A+m] - A \ln[A] \quad (4.3)$$

As can be easily seen this fulfills the renormalization condition that the first order contribution to the self-energy has to vanish at the renormalization point 0.

4.1.2 Calculation of the prefactor

To find the complete contribution to the self-energy we need to compute the combinatorial factors too. The Feynman rules give contributions for each line and vertex. The number of times a graph appears when calculating all possible contractions of the fields has to be taken into account as well.

To find this combinatorial factor one has to multiply

- the number of times the graph appears differently when rotating it
- a factor of (# of vertices)! for all possibilities to which vertex the incoming $\bar{\phi}$ or ϕ respectively, can contract
- a factor of $2^{\#ofvertices}$ or $4^{\#ofvertices}$ in the complex and real case for the legs the incoming lines can contract to

Here we have one vertex and one line in our Feynman graph which gives

$$-\tilde{\lambda}(4\pi^2\theta^2)(4\pi)^2 \frac{1}{[(4\pi)^2\theta]^2} \sum_N \frac{K_N}{4} (G_N^{(1)})_{mn} = -\frac{\tilde{\lambda}}{4} \sum_N \frac{K_N}{4} (G_N^{(1)})_{mn} \quad (4.4)$$

Here a factor $(4\pi)^2\theta$ has been taken out for convenience (see Equation (4.6)) and the sum over N runs over the different graphs. Now the combinatorial factor has to be calculated. We find

- a factor 2 for the possible appearences T_{up} and T_{down}
- a factor of 1! for the one existing vertex

- a factor of 4^1 for the possible legs the line can contract to at the vertex

As we have the sum over the different graphs in our definition of the prefactor, we leave the factor of 2 for the appearances out, and then multiplying the other factors we find that $K^r_G = 4$ in the real case and therefore the one-loop-contribution to the self-energy is

$$A_{mn} = \frac{1}{4} \sum_N (G^{(1)}_N)_{mn} \tag{4.5}$$

where the sum over N stand for the necessary 1-loop-graphs. The self energy can now be written down

$$\frac{1}{(4\pi)^2\theta}\Sigma_{mn} = -\tilde{\lambda}A_{mn} = \frac{-\tilde{\lambda}}{4}\Big(-(m+n)\ln[\Lambda] + (m+n)\ln[2]+ \\ +(A+m)\ln[A+m] + (A+n)\ln[A+n] - 2A\ln[A]\Big) \tag{4.6}$$

4.1.3 Field-strength-renormalization

We find the field-strength renomalization by differentiating the self-energy-contribution once with respect to the external momentum m or n. At first order we thus get a $\ln[\Lambda]$ -contribution to our field-strength-renormalization Z.

$$\delta Z_1 = -\partial_{m_1}(A_{mn}) = \frac{1}{4}\Big(\ln[\Lambda] + \ln[2] + \ln[A]\Big) \tag{4.7}$$

4.2 Two-loop-calculation

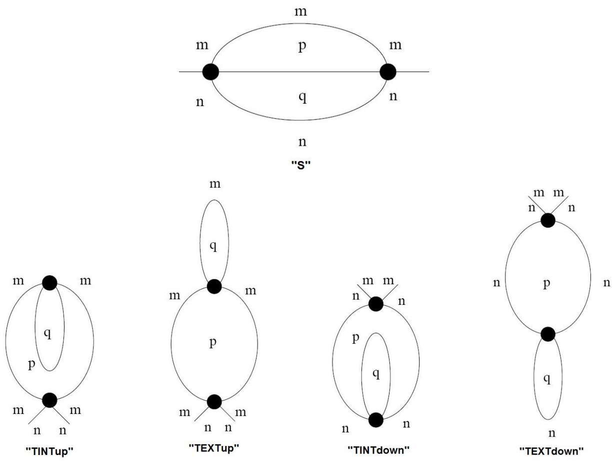

Figure 4.3: 2-loop-diagrams

At 2-loop-order we have to calculate and renormalize three different Feynman graphs, found in Figure 4.3. Each depicted graph is supposed to be a ribbon graph. The single lines are just used to simplify the diagrams itself. The corresponding amplitudes are

$$G^{S}_{mn} = \int_0^\Lambda\!\!\int_0^\Lambda \mathrm{d}^2p\,\mathrm{d}^2q \frac{1}{(A+p+m)(A+p+q)(A+q+n)} \tag{4.8}$$

$$G^{TINT_{up}}_{mn} = \int_0^\Lambda\!\!\int_0^\Lambda \mathrm{d}^2p\,\mathrm{d}^2q \frac{1}{(A+p+m)^2(A+p+q)} \tag{4.9}$$

$$G^{TEXT_{up}}_{mn} = \int_0^\Lambda\!\!\int_0^\Lambda \mathrm{d}^2p\,\mathrm{d}^2q \frac{1}{(A+p+m)^2(A+q+m)} \tag{4.10}$$

$$G^{TINT_{down}}_{mn} = \int_0^\Lambda\!\!\int_0^\Lambda \mathrm{d}^2p\,\mathrm{d}^2q \frac{1}{(A+q+n)^2(A+p+q)} \tag{4.11}$$

$$G^{TEXT_{down}}_{mn} = \int_0^\Lambda\!\!\int_0^\Lambda \mathrm{d}^2p\,\mathrm{d}^2q \frac{1}{(A+p+n)^2(A+q+n)} \tag{4.12}$$

4.2.1 Asymptotical behaviour of the divergent graphs

Analyzing the degree of divergence of the graphs we will again find quadratic and logarithmic divergences. The ocurring infinities of each diagram are as follows:

$$\begin{aligned} G^{S}_{mn}\Big|_{m=n=0} &\overset{\Lambda\to\infty}{=} \Big(-3(\ln[2])^2 + 2\ln[2]\Big)\Lambda - A(\ln[\Lambda])^2 + \\ &\quad + \Big(2A\ln[2] - A + 2A\ln[A]\Big)\ln[\Lambda] \end{aligned} \tag{4.13}$$

$$\begin{aligned} G^{TINT_{up}}_{mn}\Big|_{m=n=0} &\overset{\Lambda\to\infty}{=} \Lambda(2\ln[2]\ln[\Lambda] - 2\ln[2] + \ln[2]^2 - 2\ln[2]\ln[A+m]) + \\ &\quad + \ln[\Lambda]^2(\frac{A}{2} + m) + \ln[\Lambda](A - m - A\ln[2] - \\ &\quad - 2m\ln[2] - A\ln[A+m] - 2m\ln[A+m]) \end{aligned} \tag{4.14}$$

$$\begin{aligned} G^{TEXT_{up}}_{mn}\Big|_{m=n=0} &\overset{\Lambda\to\infty}{=} \Big(2\ln[2\Lambda] - 2(\ln[2])^2 - 2\ln[2A]\Big)\Lambda - \\ &\quad - A(\ln[\Lambda])^2 + 2A\ln[2A]\ln[\Lambda] \end{aligned} \tag{4.15}$$

4.2.2 Mass-renormalization

At this order we have to take care about subdivergences which will occur at two-loop and higher orders. Subtracting the overall divergence will not cure all divergences because just one of the loops may diverge as well. If you take, for example, the graph "TEXTup", loop q may diverge while loop p stays finite. This will produce further infinities called subdivergences. In this diagram you subtract it by substituting the tadpole q by its counterterm, which we already computed at one-loop-order (see figure 4.4).

Renormalizing the sunrise diagram ("S") is a bit more complicated because here we have to deal with so called "overlapping divergences". These are loops which have one propagator in common. Fortunately, by applying the forest-formula found by Zimmermann, this problem becomes easily tractable as well. One just has to cancel each loop containing a subdivergence by its counterterm seperately and add the necessary overall counterterms at the end. Graphically, this is shown in figure 4.5 and gives a quite good intuitive understanding of the forest formula (for details see [12]).

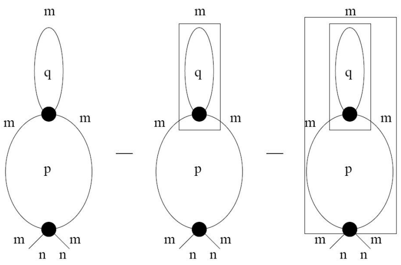

Figure 4.4: Renormalizing the “TEXTup”-graph

Actually in the “S” diagram, the only mass divergence comes from the overall counterterm. The subdivergences give contributions to the field-strength and the coupling constant renormalization. Later on, it will be argued that the coupling constant renormalization can be ignored because it just gives finite contributions. The reason it has to be taken into account here is, that the derivation of the subdivergence contributes to the field-strength as well. The subtraction renormalizing the coupling constant is not necessary.

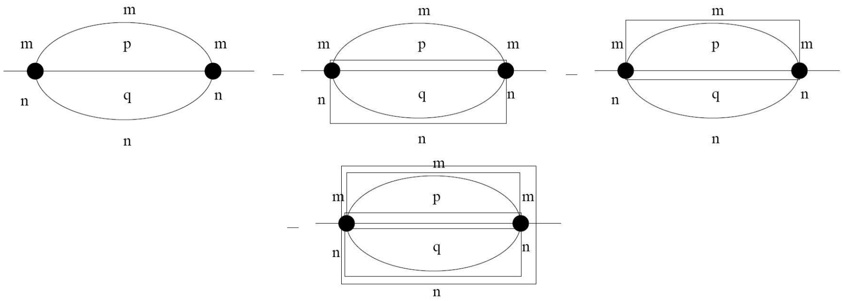

Figure 4.5: Renormalizing the Sunrise-graph

The explicit calculations of the graphs can be found in Appendix 1. Here I just state the renormalized amplitudes.

$$\begin{aligned}G^{S,R}_{mn} =& \int_0^\Lambda\!\!\int_0^\Lambda \mathrm{d}^2p\mathrm{d}^2q\Big\{\frac{1}{(A+p+m)(A+p+q)(A+q+n)}-\\ &-\frac{1}{(A+p)^2(A+q+n)}-\frac{1}{(A+p+m)(A+q)^2}-\\ &-\Big(\frac{1}{(A+p)(A+p+q)(A+q)}-\frac{1}{(A+p)^2(A+q)}-\\ &-\frac{1}{(A+p)(A+q)^2}\Big)\Big\}\end{aligned} \tag{4.16}$$

$$\begin{aligned}G^{TINT_{up},R}_{mn} =& \int_0^\Lambda\!\!\int_0^\Lambda \mathrm{d}^2p\mathrm{d}^2q\Big\{\frac{1}{(A+p+m)^2(A+p+q)}-\\ &-\frac{1}{(A+p+m)^2(A+q)}-\Big(\frac{1}{(A+p)^2(A+p+q)}-\\ &-\frac{1}{(A+p)^2(A+q)}\Big)\Big\}\end{aligned} \tag{4.17}$$

$$\begin{aligned}G^{TEXT_{up},R}_{mn} =& \int_0^\Lambda\!\!\int_0^\Lambda \mathrm{d}^2p\mathrm{d}^2q\Big\{\frac{1}{(A+p+m)^2(A+q+m)}-\\ &-\frac{1}{(A+p+m)^2(A+q)}-\Big(\frac{1}{(A+p)^2(A+q)}-\\ &-\frac{1}{(A+p)^2(A+q)}\Big)\Big\}\end{aligned} \tag{4.18}$$

$$\begin{aligned}G^{TINT_{down},R}_{mn} =& \int_0^\Lambda\!\!\int_0^\Lambda \mathrm{d}^2p\mathrm{d}^2q\Big\{\frac{1}{(A+q+n)^2(A+p+q)}-\\ &-\frac{1}{(A+q+n)^2(A+p)}-\Big(\frac{1}{(A+q)^2(A+p+q)}-\\ &-\frac{1}{(A+p)^2(A+q)}\Big)\Big\}\end{aligned} \tag{4.19}$$

$$\begin{aligned}G^{TEXT_{down},R}_{mn} =& \int_0^\Lambda\!\!\int_0^\Lambda \mathrm{d}^2p\mathrm{d}^2q\Big\{\frac{1}{(A+p+n)^2(A+q+n)}-\\ &-\frac{1}{(A+p+n)^2(A+q)}-\Big(\frac{1}{(A+p)^2(A+q)}-\\ &-\frac{1}{(A+p)^2(A+q)}\Big)\Big\}\end{aligned} \tag{4.20}$$

Here again, we have to define the combinatorial factors of the graphs. After taking out the factor of $\frac{1}{(4\pi)^2\theta}$ we have

$$\frac{1}{2!}\tilde{\lambda}^2(4\pi^2\theta^2)^2(4\pi)^4\frac{1}{[(4\pi)^2\theta]^4}\sum_N\frac{K_N}{4^2}(G^{(2)}_N)_{mn}=\frac{\tilde{\lambda}^2}{4^2}\frac{1}{2}\sum_N\frac{K_N}{4^2}(G^{(2)}_N)_{mn} \tag{4.21}$$

The combinatorial factor K_N is the same for all three graphs as we always have two vertices and three internal lines:

$$K_N = 2\cdot 4^2 \tag{4.22}$$

The two-loop-contribution is thus

$$B_{mn} = \frac{1}{4^2} \sum_N (G_N)^{(2)}_{mn} \tag{4.23}$$

and the self-energy up to 2-loop-order is

$$\Sigma_{mn} = -\tilde{\lambda} A_{mn} + \tilde{\lambda}^2 B_{mn} \tag{4.24}$$

4.2.3 Field-strength-renormalization

By differentiating these graphs once we get the two-loop-contribution to the field strength.

$$\delta Z_2 = -\frac{1}{4^2}\Big(\frac{\partial}{\partial m_1} G^{S,R}_{mn} + \frac{\partial}{\partial m_1} G^{TEXT_{up},R}_{mn} + \frac{\partial}{\partial m_1} G^{TINT_{up},R}_{mn}\Big)\Big|_{m=n=0} \tag{4.25}$$

where

$$-\frac{\partial}{\partial m_1} G^{S,R}_{mn}\Big|_{m=n=0} = \sum_{p,q}\Big(\frac{1}{(A+p)^2(A+p+q)(A+q)} - \frac{1}{(A+p)^2(A+q)^2}\Big) \tag{4.26}$$

$$-\frac{\partial}{\partial m_1} G^{TEXT_{up},R}_{mn}\Big|_{m=n=0} = \sum_{p,q}\Big(\frac{1}{(A+p)^2(A+q)^2}\Big) \tag{4.27}$$

$$-\frac{\partial}{\partial m_1} G^{TINT_{up},R}_{mn}\Big|_{m=n=0} = \sum_{p,q}\Big(\frac{2}{(A+p)^3(A+p+q)} - \frac{2}{(A+p)^3(A+q)}\Big) \tag{4.28}$$

Hence the two-loop-contribution is

$$\begin{aligned}\delta Z_2 = \frac{\tilde{\lambda}}{4^2}\Big(&-\frac{(\ln[\Lambda])^2}{2} + \ln[\Lambda](3+\ln[2]+\ln[A]) - \\ &-1 - 3\ln[2] - \frac{3(\ln[2])^2}{2} - 3\ln[A] - \ln[2]\ln[A] - \frac{\ln[A]^2}{2}\Big)\end{aligned} \tag{4.29}$$

and we get a field-strength-renormalization up to two-loop-order that is

$$\begin{aligned}Z = 1 - \frac{\tilde{\lambda}}{4}\int_0^\Lambda\!\!\int_0^\Lambda d^2p \frac{1}{(A+p)^2} + \frac{\tilde{\lambda}}{16}\int_0^\Lambda\!\!\int_0^\Lambda d^2p d^2q \Big(&\frac{2}{(A+p)^3(A+p+q)} - \\ -\frac{2}{(A+p)^3(A+q)} + \frac{1}{(A+p)^2(A+p+q)(A+q)}\Big)&\end{aligned} \tag{4.30}$$

4.3 4-pt-function

Renormalizing the 4-point-graphs you have to take care of the mass subdivergence in the BINT and BEXT diagram (figure 4.7). There are other subdivergences in the B2 and the E diagram which do contribute to the coupling constant renormalization as do all the overall divergencies of the diagrams. Because in the next section it is shown that the difference between bare and renormalized coupling is finite we are just interested in renormalizing the mass divergences and neglect the renormalization of the coupling itself. The amplitudes of the graphs, including mass renormalization, are

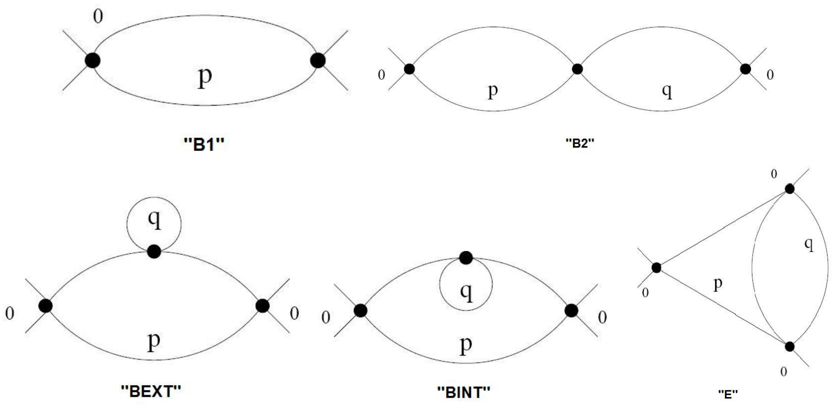

Figure 4.6: 4-pt-graphs at 1- and 2-loop-order

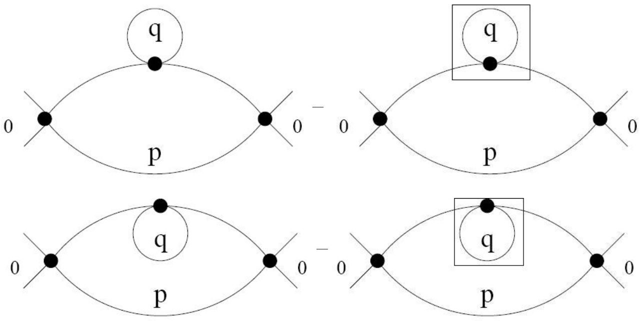

Figure 4.7: Mass-renormalizing the 4-point-graphs

$$G^{B1}(0,0,0,0) = \int_0^\Lambda \mathrm{d}^2p\mathrm{d}^2q \frac{1}{(A+p)^2} \tag{4.31}$$

$$G^{B2}(0,0,0,0) = \int_0^\Lambda\int_0^\Lambda \mathrm{d}^2p\mathrm{d}^2q \frac{1}{(A+p)^2(A+q)^2} \tag{4.32}$$

$$G^{BEXT}(0,0,0,0) = \int_0^\Lambda\int_0^\Lambda \mathrm{d}^2p\mathrm{d}^2q \Big\{ \frac{1}{(A+p)^3(A+q)} - \frac{1}{(A+p)^3(A+q)} \Big\} \tag{4.33}$$

$$G^{BINT}(0,0,0,0) = \int_0^\Lambda\int_0^\Lambda \mathrm{d}^2p\mathrm{d}^2q \Big\{ \frac{1}{(A+p)^3(A+p+q)} - \frac{1}{(A+p)^3(A+q)} \Big\} \tag{4.34}$$

$$G^{E}(0,0,0,0) = \int_0^\Lambda\int_0^\Lambda \mathrm{d}^2p\mathrm{d}^2q \frac{1}{(A+p)^2(A+p+q)(A+q)} \tag{4.35}$$

The graph BEXT is completely canceled by its mass-counterterm and vanishes. The other graphs have to be calculated.

The one-loop-graph B1 has two vertices and two lines and a factor of 1/2! which comes from the exponential of the action in perturbation theory. The coefficient of the

4-pt-function is thus given by

$$a' = \frac{1}{8}\frac{K(B1)}{4^2}G^{B1} \quad \text{with} \quad K(B1) = 4^3$$
$$\longrightarrow a' = \frac{1}{2}\frac{1}{(A+p)^2} = \frac{1}{2}\Big(\ln[\Lambda] + \ln[2] + \ln[A]\Big) \tag{4.36}$$

In the two-loop-case there are three vertices and four internal lines and so

$$b' = \frac{1}{3!4^2}\sum_N \frac{K(N)}{4^3}S_N \tag{4.37}$$

The combinatorial factors are

$$K(E) = K(BEXT) = K(BINT) = 3!\cdot 4^3 \cdot 4, \qquad K(B2) = 3!\cdot 4^3\cdot 2. \tag{4.38}$$

Having computed the amplitudes of the Feynman graphs and the combinatorial factors we have to take a look how many times the diagrams appear. Like in the case of the 2-point-graphs, the loops can “look” in different directions and therefore affect different external indices. Taking the “BEXT” graph as an example, this graph has a counterpart where the tadpole lies at the lower border of the loop p. The difference between these two diagrams obviously vanishes when the external indices are set to zero but this means the amplitude of this graphs give a factor two in our calculation of the coefficient of the 4-point-function. The graphs “BINTup” and “E” appear twice as well and so finally the 2-loop-coefficient of Γ^4 adds up to

$$\begin{aligned}
b' &= \frac{1}{8}\Big(G^{B2} + 2(G^{E} + G^{BEXT} + G^{BINT})\Big) = \\
&= \frac{1}{8}\Big(\frac{1}{(A+p)^2(A+q)^2} + \frac{2}{(A+p)^3(A+p+q)} + \\
&\qquad \frac{2}{(A+p)^2(A+p+q)(A+q)} - \frac{2}{(A+p)^3(A+q)}\Big) = \\
&= \frac{1}{8}\Big(\ln[\Lambda]^2 + \ln[\Lambda](3 - 2\ln[A] + 2\ln[2]) - \\
&\qquad - 2 - 3\ln[2A] + \ln[2]^2 + 2\ln[2]\ln[A] + \ln[A]^2\Big)
\end{aligned} \tag{4.39}$$

Thus the complete 4-point-function is given by

$$\begin{aligned}
\Gamma^4(0,0,0,0) = 1 &- \frac{\tilde{\lambda}}{2}\int_0^\Lambda\!\!\int_0^\Lambda \mathrm{d}^2p\mathrm{d}^2q\frac{1}{(A+p)^2} + \\
&+ \frac{\tilde{\lambda}^2}{8}\int_0^\Lambda\!\!\int_0^\Lambda \mathrm{d}^2p\mathrm{d}^2q\Big(\frac{1}{(A+p)^2(A+q)^2} + \frac{2}{(A+p)^3(A+p+q)} + \\
&\qquad \frac{2}{(A+p)^2(A+p+q)(A+q)} - \frac{2}{(A+p)^3(A+q)}\Big)
\end{aligned} \tag{4.40}$$

Chapter 5

Boundedness of β-function

With the results from the last section it can be shown that the difference of the renormalized and the bare coupling constant is just finite and thus the beta-function bounded. Thus we will just worry about the infinite factors of graphs in this section.

To compute the evolution equation of the effective coupling we need the 4-pt-function with the external indices set to zero and the corresponding wave-function renormalization. It is given up to 2-loops by

$$\begin{aligned} Z &= 1 - a\tilde{\lambda} + b\tilde{\lambda}^2 = \\ &= 1 - \frac{\tilde{\lambda}}{4}\ln[\Lambda] + \frac{\tilde{\lambda}^2}{4^2}\Big(-\frac{1}{2}\ln[\Lambda]^2 - \ln[\Lambda](3 + \ln[A] + \ln[2])\Big) \end{aligned} \tag{5.1}$$

The 4-point-function is

$$\Gamma^4(0,0,0,0) = -\lambda(4\pi^2\theta^2)(1 - a'\tilde{\lambda} + b'\tilde{\lambda}^2) \tag{5.2}$$

The evolution equation of the coupling constant is, as already stated earlier,

$$\lambda_r = -\frac{1}{4\pi^2\theta^2}\frac{\Gamma_4(0,0,0,0)}{Z^2} \tag{5.3}$$

Now the functions calculated above are expanded up to two-loop-order

$$\frac{1 - a'\tilde{\lambda} + b'\tilde{\lambda}^2}{(1 - a\tilde{\lambda} + b\tilde{\lambda}^2)^2} = 1 - \gamma_1\tilde{\lambda} + \gamma_2\tilde{\lambda}^2 \tag{5.4}$$

Now this equation is multiplied by Z^2 and expanded

$$\begin{aligned} \longrightarrow 1 - a'\tilde{\lambda} + b'\tilde{\lambda}^2 &= (1 - \gamma_1\tilde{\lambda} + \gamma_2\tilde{\lambda}^2)(1 - a\tilde{\lambda} + b\tilde{\lambda}^2) \\ &= (1 - \gamma_1\tilde{\lambda} + \gamma_2\tilde{\lambda}^2)(1 + a^2\tilde{\lambda}^2 + b^2\tilde{\lambda}^4 - 2a\tilde{\lambda} + 2b\tilde{\lambda}^2 - 2ab\tilde{\lambda}^3) \\ &= 1 - \gamma_1\tilde{\lambda} - 2a\tilde{\lambda} + 2a\gamma_1\tilde{\lambda} + a^2\tilde{\lambda}^2 + 2b\tilde{\lambda}^2 + \gamma_2\tilde{\lambda}^2 + 2a\gamma_1\tilde{\lambda}^2 + O(\tilde{\lambda}^3) \end{aligned} \tag{5.5}$$

5.1 First-order-contribution

Comparing the first order terms in λ we find

$$\begin{aligned} a' &= \gamma_1 + 2a \\ \frac{1}{2}\ln[\Lambda] &= \gamma_1 + \frac{1}{2}\ln[\Lambda] \quad \longrightarrow \quad \gamma_1 = 0 \end{aligned} \tag{5.6}$$

"a'" being the coefficient of the 4-point-function and "a" the 2-point-coefficient. Hence, the first-order-contribution to the coupling constant vanishes.

5.2 Second-order-contribution

For clearness the independent integrals are renamed as follows

$$\begin{aligned} &\int_0^\Lambda\!\!\int_0^\Lambda \mathrm{d}^2p\mathrm{d}^2q \frac{1}{(A+p)^2} = S_1^{(1)} \\ &\int_0^\Lambda\!\!\int_0^\Lambda \mathrm{d}^2p\mathrm{d}^2q \frac{1}{(A+p)^2(A+q)^2} = S_1^{(2)} = (S_1^{(1)})^2 \\ &\int_0^\Lambda\!\!\int_0^\Lambda \mathrm{d}^2p\mathrm{d}^2q \frac{1}{(A+p)^2(A+p+q)(A+q)} = S_2^{(2)} \\ &\int_0^\Lambda\!\!\int_0^\Lambda \mathrm{d}^2p\mathrm{d}^2q \frac{1}{(A+p)^3(A+q)} = S_3^{(2)} \\ &\int_0^\Lambda\!\!\int_0^\Lambda \mathrm{d}^2p\mathrm{d}^2q \frac{1}{(A+p)^3(A+p+q)} = S_4^{(2)} \end{aligned} \tag{5.7}$$

The second-order-contribution to the 4-point-function and the wave function are written with this shortcuts

$$\begin{aligned} b &= \frac{1}{16}(S_2^{(2)} + 2S_3^{(2)} + 2S_4^{(2)}) \\ b' &= \frac{1}{8}(S_1^{(2)} + 2S_2^{(2)} + 2S_3^{(2)} + 2S_4^{(2)}) \end{aligned} \tag{5.8}$$

Now putting the coefficients into the second-order-contribution of the evolution equation it is found that

$$\begin{aligned} b' &= a^2 + 2b + \gamma_2 \\ \frac{1}{8}(S_1^{(2)} + 2S_2^{(2)} + 2S_3^{(2)} + 2S_4^{(2)}) &= (\frac{1}{4}S_1^{(1)})^2 + \frac{1}{8}(2S_4^{(2)} - 2S_3^{(2)} + S_2^{(2)}) + \gamma_2 \end{aligned} \tag{5.9}$$

and

$$\begin{aligned}
\gamma_2 &= \frac{1}{16}(2S_2^{(2)} + S_1^{(2)}) = \\
&= \int_0^\Lambda\!\!\int_0^\Lambda \mathrm{d}^2p\mathrm{d}^2q\Big(\frac{1}{(A+p)^2(A+p+q)(A+q)} - \frac{1}{(A+p)^2(A+q)^2}\Big) = \\
&= \int_0^\Lambda\!\!\int_0^\Lambda \mathrm{d}^2p\mathrm{d}^2q\frac{A+p-q}{(A+p)^2(A+p+q)(A+q)^2} = \\
&= A\int_0^\Lambda\!\!\int_0^\Lambda \mathrm{d}^2p\mathrm{d}^2q\frac{1}{(A+p)^2(A+p+q)(A+q)^2}
\end{aligned} \tag{5.10}$$

which is finite as can be seen by taking a look at the order of divergence. “p” has dimension 2 and order 3, therefore it is finite. Exactly the same happens with “q”. It is thus proven that, up to two loop order, the evolution of the coupling constant is bounded.

Chapter 6

Vanishing Of Beta-Function Up To All Orders

The proof of a vanishing beta-function up to all order was done by Rivasseau et. al. in [10] at the self dual point $\Omega = 1$. It relies on Ward-Identities and the Dyson-Schwinger-Equation which are combined to give a proof of the theorem stated in section 2 (see Equation (2.10)). The detailed steps will be followed below. Here the complex Grosse-Wulkenhaar-model will be used.

First the generating functional is defined:

$$\begin{aligned} Z(\eta,\bar\eta) &= \int \mathrm{d}\phi\mathrm{d}\bar\phi e^{-S(\phi,\bar\phi)+F(\eta,\bar\eta,\phi,\bar\phi)} \\ F(\eta,\bar\eta,\phi,\bar\phi) &= \bar\phi\eta + \bar\eta\phi \\ S(\phi,\bar\phi) &= \bar\phi X\phi + \phi X\bar\phi + A\bar\phi\phi + \frac{\lambda}{2}\phi\bar\phi\phi\bar\phi \end{aligned} \tag{6.1}$$

Here X stands for $m\delta_{mn}$, S for the action and F is the external source. First, the Ward Identities will be worked out.

6.1 The Ward Identities

As the complex model is used, the propagators are oriented. This means that the incoming line is given by a $\bar\phi$ and the outgoing lines by a ϕ. For a field $\bar\phi_{ab}$ the index a is called a left index and b a right one. The first index of a field $\bar\phi$ contracts with the second index of a ϕ.

Starting to variate the action we define $U = e^{iB}$ where B is the infinitesimal generator, here a hermitian matrix. It can act from the "left" and from the "right" side, which means acting on the left, or respectively on the right, index. Here just the left action will be considered.

$$\phi^U = \phi U \qquad \bar\phi^U = U^\dagger\bar\phi \tag{6.2}$$

Expanding up to first order and variating the action gives

$$\begin{aligned} \delta S &= \phi U X U^\dagger\bar\phi - \phi X\bar\phi \approx \phi(1+iB)X(1-iB)\bar\phi - \phi X\bar\phi = \\ &= \phi X\bar\phi + i\phi BX\bar\phi - i\phi XB\bar\phi - \phi X\bar\phi = i(\phi BX\bar\phi - \phi XB\bar\phi) = \\ &= iB(X\bar\phi\phi - \bar\phi\phi X) \end{aligned} \tag{6.3}$$

The external source has to be variated as well.

$$\begin{aligned} \delta F =& U^\dagger \bar{\phi}\eta - \bar{\phi} + \bar{\eta}\phi U - \bar{\eta}\phi \approx -iB\bar{\phi}\eta + i\bar{\eta}\phi B = \\ =& iB(-\bar{\phi}\eta + \bar{\eta}\phi) \end{aligned} \tag{6.4}$$

Minimizing the generating functional leads to:

$$\begin{aligned} \frac{\delta \ln Z}{\delta A_{ab}} = 0 =& \frac{1}{Z(\bar{\eta},\eta)} \int \mathrm{d}\bar{\phi}\mathrm{d}\phi \Big(-\frac{\delta S}{\delta A_{ab}} + \frac{\delta F}{\delta A_{ab}} \Big) e^{-S+F} = \\ =& \frac{1}{Z(\bar{\eta},\eta)} \int \mathrm{d}\bar{\phi}\mathrm{d}\phi \Big(-[X\bar{\phi}\phi - \bar{\phi}\phi X]_{ab} + [-\bar{\phi}\eta + \bar{\eta}\phi]_{ab} \Big) \end{aligned} \tag{6.5}$$

Now we derivate with respect to the external source $\partial_\eta \partial_{\bar{\eta}}|_{\eta=\bar{\eta}=0}$ and therefore get the 2-point Green's function which we want to minimize. Here the external source is set to zero for convenience.

$$\begin{aligned} 0 =& < \partial_\eta \partial_{\bar{\eta}} (-[X\bar{\phi}\phi - \bar{\phi}\phi X]_{ab} + [-\bar{\phi}\eta + \bar{\eta}\phi]_{ab} e^{F(\eta,\bar{\eta})})|_0 >_c = \\ =& < \frac{\partial(\bar{\eta}\phi)_{ab}}{\partial\bar{\eta}} \frac{\partial(\bar{\phi}\eta)}{\partial\eta} - \frac{\partial(\bar{\phi}\eta)_{ab}}{\partial\eta} \frac{\partial(\bar{\eta}\phi)}{\partial\bar{\eta}} - [X\bar{\phi}\phi - \bar{\phi}\phi X]_{ab} \frac{\partial(\bar{\eta}\phi)}{\partial\bar{\eta}} \frac{\partial(\bar{\phi}\eta)}{\partial\eta} >_c \end{aligned} \tag{6.6}$$

Because $X = m\delta_{mn}$, we can write the correlation function as

$$(a-b) < [\bar{\phi}\phi]_{ab} \frac{\partial(\bar{\eta}\phi)}{\partial\bar{\eta}} \frac{\partial(\bar{\phi}\eta)}{\partial\eta} >_c = < \frac{\partial(\bar{\eta}\phi)_{ab}}{\partial\bar{\eta}} \frac{\partial(\bar{\phi}\eta)}{\partial\eta} >_c - < \frac{\partial(\bar{\phi}\eta)_{ab}}{\partial\eta} \frac{\partial(\bar{\eta}\phi)}{\partial\bar{\eta}} >_c \tag{6.7}$$

If we set $\eta = \eta_{\nu\mu}$ and $\bar{\eta} = \bar{\eta}_{\beta\alpha}$ we receive

$$(a-b) < [\bar{\phi}\phi]_{ab} \phi_{\alpha\beta} \bar{\phi}_{\mu\nu} >_c = < \delta_{\alpha\beta} \phi_{\alpha b} \bar{\phi}_{\mu\nu} >_c - < \delta_{b\mu} \bar{\phi}_{a\nu} \phi_{\alpha\beta} >_c \tag{6.8}$$

Because the power-counting shows that the only relevant graphs have one external face and genus 0 (see [3]) we can set

$$\alpha = \nu \qquad a = \beta \qquad b = \mu$$

and hence, get the Ward Identity for the 2-point-function:

$$(a-b) < [\bar{\phi}\phi]_{ab} \phi_{\nu a} \bar{\phi}_{b\nu} >_c = < \phi_{\nu b} \bar{\phi}_{b\nu} >_c - < \bar{\phi}_{a\nu} \phi_{\nu a} >_c \tag{6.9}$$

To find the Ward Identities for the 4-point-function we have to derivate once more after η and $\bar{\eta}$ and repeat the procedure.

$$\begin{aligned} & (a-b) < [\bar{\phi}\phi]_{ab} \partial_{\bar{\eta}_1}(\bar{\eta}\phi) \partial_{\bar{\eta}_1}(\bar{\phi}\eta) \partial_{\bar{\eta}_2}(\bar{\eta}\phi) \partial_{\bar{\eta}_2}(\bar{\phi}\eta) >_c = \\ & = < \partial_{\bar{\eta}_1}(\bar{\eta}\phi) \partial_{\bar{\eta}_1}(\bar{\phi}\eta) [\partial_{\bar{\eta}_2}(\bar{\eta}\phi) \partial_{\bar{\eta}_2}(\bar{\phi}\eta) - \partial_{\bar{\eta}_2}(\bar{\phi}\eta) \partial_{\bar{\eta}_2}(\bar{\eta}\phi)] >_c + (1 \leftrightarrow 2) \end{aligned} \tag{6.10}$$

With $\bar{\eta}_{1,\beta\alpha}$, $\eta_{1,\nu\mu}$, $\bar{\eta}_{2,\delta\gamma}$, $\eta_{2,\sigma\rho}$ we get

$$\begin{aligned} & (a-b) < [\bar{\phi}\phi]_{ab} \phi_{\alpha\beta} \bar{\phi}_{\mu\nu} \phi_{\gamma\delta} \bar{\phi}_{\rho\sigma} >_c = \\ & = < \phi_{\alpha\beta} \bar{\phi}_{\mu\nu} \delta_{a\delta} \phi \gamma b \bar{\phi}_{\rho\sigma} >_c - < \phi_{\alpha\beta} \bar{\phi}_{\mu\nu} \phi \gamma \delta \bar{\phi}_{a\sigma} \delta_{b\rho} >_c + \\ & + < \phi_{\gamma\delta} \bar{\phi}_{\rho\sigma} \delta_{a\beta} \phi \alpha b \bar{\phi}_{\mu\nu} >_c - < \phi_{\gamma\delta} \bar{\phi}_{\rho\sigma} \phi \alpha \beta \bar{\phi}_{a\nu} \delta_{b\mu} >_c \end{aligned} \tag{6.11}$$

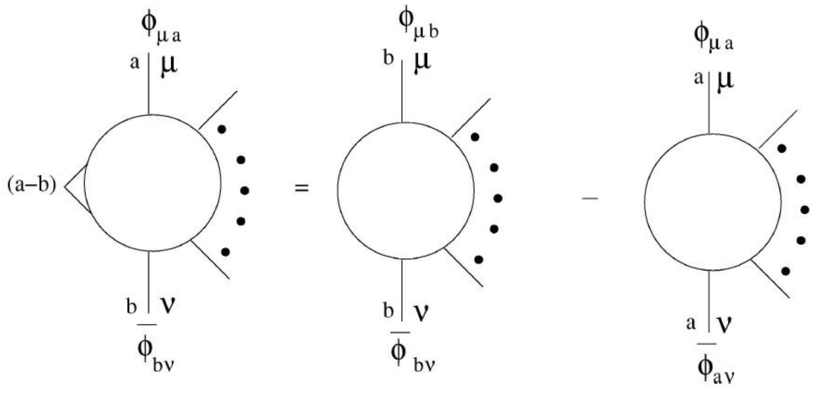

Figure 6.1: Ward Identity for 2p-point-functions with a left insertion

Again, by just taking care of the planar graphs with one external face

$$\alpha = \sigma \qquad \beta = a \qquad b = \mu \qquad \nu = \gamma \qquad \delta = \rho$$

and we get the Ward Identity:

$$(a-b) < \phi_{\alpha a}[\bar\phi\phi]_{ab}\bar\phi_{b\nu}\phi_{\nu\delta}\bar\phi_{\delta\alpha} >_c = < \phi_{\alpha b}\bar\phi_{b\nu}\phi_{\nu\delta}\bar\phi_{\delta\alpha} >_c - < \phi_{\alpha a}\bar\phi_{a\nu}\phi_{\nu\delta}\bar\phi_{\delta\alpha} >_c \qquad (6.12)$$

Obviously this procedure could be continued to get Ward Identities for higher 2n-point-functions. Further, these identities give connections between 2n- and $(2n-2)$-point functions which permit to express a 2n-point-function as the difference of two $(2n-2)$-point-functions. Explicitly, this is done in section 7.

There can be obtained similar identities by using the "right" unitary transformation and therefore receive an insertion on the "right" face.

6.2 Proof of the Theorem

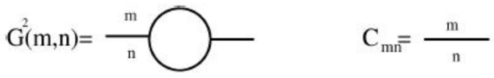

Figure 6.2: The dressed propagator $G^2(m,n) = \frac{1}{C_{mn}^{-1} - \Sigma(m,n)}$ and the bare one $C_{mn} = \frac{1}{A+m+n}$

Before the actual proof is started, some notations are explained. We use the same notation for the 4-point-function as before, namely $G^4(m,n,k,l)$ but differentiate between the bare and the dressed 2-point-function as indicated in figure 6.2. Further, a single-border function with one insertion will be needed and marked by $G_{ins}(a,b;..)$.

The break of the left-right symmetry is introduced as we are working with a "right" insertion. For a "left" one, the indices "m" and "0" would have to be exchanged. The proof can be done either in the bare, or in the mass-renormalized case. Here, the mass-renormalized theory will be used which means that $A_{ren} = A_{bare} - \Sigma(0,0)$.

This proof makes extensive use of the Dyson-Schwinger-Equation, which is the QF-theoretical generalization of the Euler-Lagrange-Equations. It expresses the classical

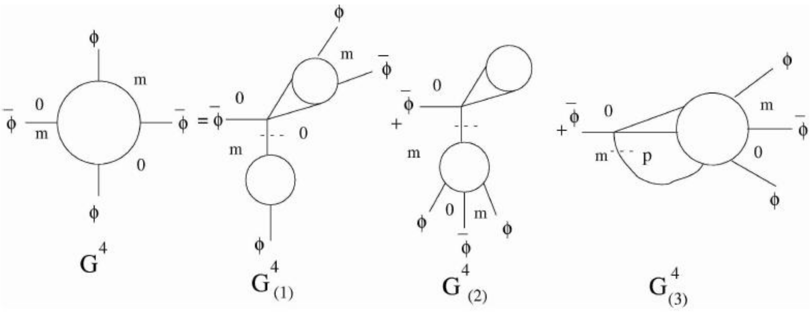

Figure 6.3: The left Dyson-Schwinger-Equation

equations of motion together with contact terms, where two fields are given at the same space-time point.

Here only the graphical illustration is needed to classify the Feynman diagrams into "generalized" ones, which represent groups of similar diagrams which can be treated together on a general level. Let's start by taking the most general 4-point-function (see left hand side of Figure 6.3) and move along the incoming line $\bar{\phi}$ on the left until the first vertex. Now move to the "right" internal line and cut this propagator. There are two possibilities what can happen now:

- the diagram can fall into two pieces or
- the diagram stays as one which means that this line was part of a loop.

This "groups of diagrams" take into account all the combinatorical factors as all graphs of one group have the same one. Moreover, setting one index to m and the other to 0 distinguishes between the graphs $G^4_{(1)}$ and $G^4_{(2)}$ and their counterparts which are included in $G^4_{(3)}$.

The first case can be identified with the first two graphs of the left side in figure 6.3. Here again two cases have to be distinguished. The graph may fall apart into a 4- and a 2-point-function or vice versa. As there can't be a one-point-function, these are the only possibilites.

If we take a closer look at $G^4_{(2)}$ we find that there is a tadpole on the upper border where the external index is set to zero. Because we are calculating in the mass-renormalized case, we immediately see that this diagram is zero after renormalization. The bare tadpole with external index set to zero gives exactly the same contribution as it's counterterm and thus, they add up to zero. The only two generalized graphs left are therefore $G^4_{(1)}$ and $G^4_{(3)}$.

6.2.1 Graph $G^4_{(1)}$

First $G^4_{(1)}$ will be analyzed. It has the form

$$G^4_{(1)} = \lambda C_{0m} G^2(0,m) G^2_{ins}(0,0;m) \tag{6.13}$$

Here, the upper 4-point-function will be interpreted as a 2-point-function with an insertion (see Figure 6.4). To be able to define the Ward Identity the index on the right side of the insertion will be set to a non-zero value ξ and the limit taken to zero afterwards.

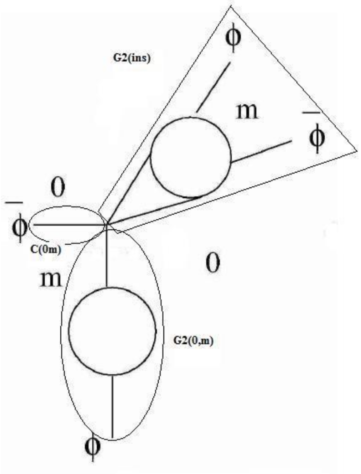

Figure 6.4: Structure of $G^4_{(1)}$ graph

Now the Identity for this graph can be given by

$$\begin{aligned} G^2_{ins}(0,0;m) &= \lim_{\xi\to 0} G^2_{ins}(\xi,0;m) = \lim_{\xi\to 0} \frac{G^2(0,m)-G^2(\xi,m)}{\xi} = \\ &= -\partial_L G^2(0,m) \end{aligned} \tag{6.14}$$

where ∂_L stands for differentiation with respect to the left index. In the case that there is no difference between the derivation with respect to the left and right index, it will be written without any index. Further, for the bare propagator differentiated by the left or the right index gives 1,

$$\partial_L C^{-1}_{ab} = \partial_R C^{-1}_{ab} = \partial C^{-1}_{ab} = 1,$$

and $G^2(0,m) = [C^{-1}_{0m} - \Sigma(0,m)]^{-1}$. So we can write

$$-\partial_L G^2(0,m) = (C^{-1}_{0,m} - \Sigma(0,m))^{-2}(1 - \partial_L \Sigma(0,m)) \tag{6.15}$$

and thus, $G^4_{(1)}$ as

$$\begin{aligned} G^4_{(1)}(0,m,0,m) &= \lambda C_{0m} \frac{C_{0m}C^2_{0m}(1-\partial_L\Sigma(0,m))}{(1-C_{0m}\Sigma(0,m))(1-C_{0m}\Sigma(0,m))^2} = \\ &= \lambda (G^2(0,m))^4 \frac{C_{0m}}{G^2(0,m)}(1-\partial_L\Sigma(0,m)) \end{aligned} \tag{6.16}$$

We can express the self-energy up to irrelevant terms as

$$\Sigma(m,n) = \Sigma(0,0) + (m+n)\partial_L\Sigma(0,0) \tag{6.17}$$

This is correct because the self-energy has diverging terms independent of the external indices, which are included in the $\Sigma(0,0)$ term and divergences which depend on m or n, included in the derivation-term and no others. Of course, $\partial_L\Sigma(0,0)$ should be understood as $\partial_L\Sigma(m,n)|_{m=n=0}$.

With this expression for the self-energy $G^2(0,m)$ can be written as

$$G^2(0,m) = \frac{1}{m + A_{bare} - \Sigma(0,m)} = \frac{1}{m[1 - \partial\Sigma(0,0)] + A_{ren}} \tag{6.18}$$

and

$$\begin{aligned} \frac{C_{0m}}{G^2(0,m)} &= \frac{m(1-\partial\Sigma(0,0)) + A^R}{m + A^R} = \\ &= \frac{(m + A^R)(1 - \partial\Sigma(0,0) + A^R - A^R + A^R\partial\Sigma(0,0)}{m + A^R} = \\ &= 1 - \partial\Sigma(0,0) + \frac{A^R\partial\Sigma(0,0)}{m + A^R} \end{aligned} \tag{6.19}$$

Here $C_{0m}^{-1} = m + A^R$. The substituion of A^R for A_{bare} is allowed because C_{0m} symbolises the incoming, free propagator in $G^4_{(1)}$ which has no divergence anyway and therefore the values are equivalent.

So finally, the result for $G^4_{(1)}$ can be written down:

$$\begin{aligned} G^4_{(1)}(0,m,0,m) = \lambda(G^2(0,m))^4(1 - \partial\Sigma(0,0) + \frac{A^R}{m + A^R}\partial\Sigma(0,0)) \\ (1 - \partial_L\Sigma(0,m)) \end{aligned} \tag{6.20}$$

6.2.2 Graph $G^4_{(3)}$

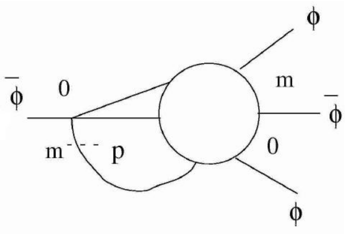

Figure 6.5: Structure of $G^4_{(3)}$ graph

Graph $G^4_{(3)}$ is not split by cutting the line so it has to be part of a loop. The Green's function for the bare values would be

$$G^{4,bare}_{(3)} = C_{0m} \sum_p G^{4,bare}_{ins}(p, 0; m, 0, m) \tag{6.21}$$

Going to the renormalized equation we have to take some more care about opening the loop. This loop would of course have a corresponding counterterm to cancel the divergence induced by p going to infinity. This counterterm vanishes if we open the loop. So we have to add this missing counterterm to receive a correct representation of graph $G^4_{(3)}$. In figure 6.6 a 1PI contribution has been pulled out of the general interaction but this does not change the calculation. We receive

$$G^4_{(3)} = C_{0m} \sum_p G^4_{ins}(0, p; m, 0, m) - C_{0m}(CT_{lost})G^4(0, m, 0, m) \tag{6.22}$$

for graph $G^4_{(3)}$ with one loop interpreted as an insertion.

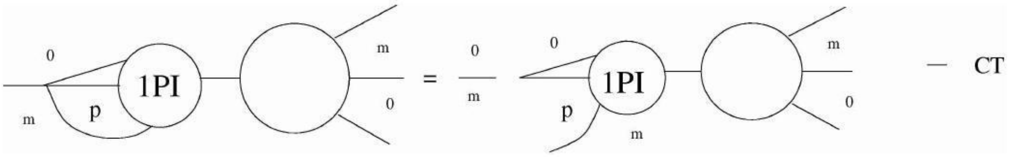

Figure 6.6: Structure of $G^4_{(3)}$ graph with missing counterterm

Not all loops which correspond to a 1PI 2 point insertion are lost when opening the loop. Obviously all loops which have just a contribution to the left index side are not affected. This is represented by a generalized left tadpole. Thus, we split the self-energy into the left tadpole contribution and the lost 2-point 1PI insertions which shall be called $\Sigma^R(m,n)$.

$$\Sigma(m,n) = T^L(m,n) + \Sigma^R(m,n) \tag{6.23}$$

As the generalized left tadpole has no contribution to the right index side, the derivation with respect to the right index will vanish. Therefore

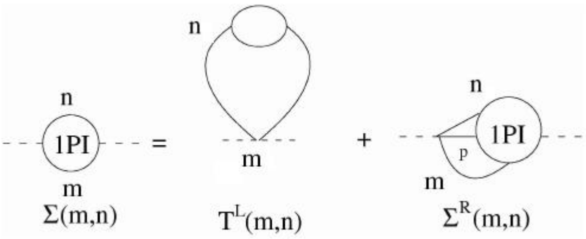

Figure 6.7: Self-energy split into generalized left tadpole and a part including contributions to right index side

$$\partial_R \Sigma^R(m,n) = \partial_R \Sigma(m,n) = \partial \Sigma(m,n) \tag{6.24}$$

The missing mass counterterm can be written as

$$CT_{lost} = \Sigma^R(0,0) = \Sigma(0,0) - T^L \tag{6.25}$$

When evaluating the lost part of the self-energy Σ^R we cut the propagator between the 1PI part and the general 4-point-function in figure 6.6 and use the Ward Identity to find:

$$\begin{aligned}\Sigma^R(0,0) &= \frac{1}{G^2(0,0)}\sum_p G^2_{ins}(0,p;0) = \frac{1}{G^2(0,0)}\sum_p \frac{1}{p}(G^2(0,0) - G^2(p,0)) = \\ &= \sum_p \frac{1}{p}\Big(1 - \frac{G^2(p,0)}{G^2(0,0)}\Big)\end{aligned} \tag{6.26}$$

So graph $G^4_{(3)}$ can be expressed as

$$\begin{aligned}G^4_{(3)}(0,m,0,m) = C_{0m}\sum_p G^4_{ins}(0,p;m,0,m) - \\ - C_{0m}G^4(0,m,0,m)\sum_p \frac{1}{p}\Big(1 - \frac{G^2(p,0)}{G^2(0,0)}\Big)\end{aligned} \tag{6.27}$$

Now the 4-point-function with the insertion can be reexpressed as well with the aid of the Ward Identity to find

$$C_{0m}\sum_p G^4_{ins}(0,p;m,0,m) = C_{0m}\sum_p \frac{1}{p}(G^4(0,m,0,m) - G^4(p,m,0,m)) \tag{6.28}$$

The second term in this equation is proportional to $\frac{1}{p^3}$ and thus finite. So we can ignore it and substituting the rest of equation (6.28) into equation (6.27) we receive

$$G^4_{(3)} = C_{0m}\frac{G^4(0,m,0,m)}{G^2(0,0)}\sum_p \frac{G^2(p,0)}{p} \tag{6.29}$$

Evaluating the sum over p we use

$$G^2(0,m) = \frac{1}{m(1-\partial\Sigma(0,0)+A^R}$$

to rewrite it as

$$\begin{aligned}\sum_p \frac{G^2(p,0)}{p} &= \sum_p \frac{G^2(p,0)}{p}\Big(1\cdot(1-\partial\Sigma(0,0)) + A^R - \\ &\quad - 0\cdot(1-\partial\Sigma(0,0)) - A^R\Big)\frac{1}{1-\partial\Sigma(0,0)} = \\ &= \sum_p \frac{G^2(p,0)}{p}\Big(\frac{1}{G^2(0,1)} - \frac{1}{G^2(0,0)}\Big)\end{aligned} \tag{6.30}$$

Repeating the steps in equation (6.26) for $\Sigma^R(0,1)$ and neglecting the irrelevant index jump from $(p,1)\to(p,0)$, for it just leaves out finite terms, we have:

$$\Sigma^R(0,1) = \sum_p \frac{1}{p}\Big(1 - \frac{G^2(p,1)}{G^2(0,1)}\Big) = \sum_p \frac{1}{p}\Big(1 - \frac{G^2(p,0)}{G^2(0,1)}\Big) \tag{6.31}$$

Now the sum over p can be written as

$$\begin{aligned}\sum_p \frac{G^2(p,0)}{p} &= (-\Sigma^R(0,1) + \frac{1}{p} + \Sigma^R(0,0) - \frac{1}{p})\frac{1}{1-\partial\Sigma(0,0)} = \\ &= \frac{\Sigma^R(0,0)-\Sigma^R(0,1)}{1-\partial\Sigma(0,0)} = \frac{-\partial_R\Sigma^R(0,0)}{1-\partial\Sigma(0,0)} = \\ &= \frac{-\partial\Sigma(0,0)}{1-\partial\Sigma(0,0)}\end{aligned} \tag{6.32}$$

So, finally

$$\begin{aligned}G^4_{(3)}(0,m,0,m) &= -C_{0m}G^4(0,m,0,m)\frac{1}{G^2(0,0)}\frac{\partial\Sigma(0,0)}{1-\partial\Sigma(0,0)} = \\ &= -G^4(0,m,0,m)\frac{A^R\partial\Sigma(0,0)}{(m+A^R)(1-\partial\Sigma(0,0))}\end{aligned} \tag{6.33}$$

with $C^{-1}_{0m} = m + A^R$ and $(G^2(0,0))^{-1} = A^R$.

6.2.3 Result

Now, that the different generalized graphs are computed, we can write down the complete 4-point-function:

$$G^4(0,m,0,m) = G^4_{(1)} + G^4_{(3)}$$

$$\Rightarrow G^4(0,m,0,m)\Big(1 + \frac{A^R}{(m+A^R)(1-\partial\Sigma(0,0))}\partial\Sigma(0,0)\Big) = \qquad (6.34)$$

$$\lambda_{bare}(G^2(0,m))^4\Big(1 - \partial\Sigma(0,0) + \frac{A^R}{m+A^R}\partial\Sigma(0,0)\Big)(1-\partial_L\Sigma(0,m))$$

$G^4_{(3)}$ has been put on the left hand side of the equation. Now the equation is multiplied by $(1-\partial\Sigma(0,0)$ and it is easily seen that the terms in the big brackets cancel to give

$$G^4(0,m,0,m) = \lambda_{bare}(G^2(0,m))^4(1-\partial_L\Sigma(0,m))(1-\partial\Sigma(0,0)) \qquad (6.35)$$

Finally we need to amputate four times to proof the theorem. As all divergences are included in $\partial\Sigma(0,0)$ we can ignore the difference between this term and $\partial\Sigma(0,m)$. Furthermore the difference $\Gamma^4(0,m,0,m) - \Gamma^4(0,0,0,0)$ is irrelevant as well and the equation that had to be proven is received:

$$\Gamma^4(0,0,0,0) = \lambda(1-\partial\Sigma(0,0))^2 \qquad (6.36)$$

Chapter 7

Explicit Calculation of Ward Identities

The Ward Identities used in the general proof of the boundedness of the beta-function give relations between 2n- and (2n-2)-point functions which are of course valid in the bare and the renormalized case. Here, these relations will be calculated explicitly for the relations between 4- and 2-point functions in the mass-renormalized case up to two-loop-level. This will give us another possiblity to show the boundedness of the beta-function as the equivalence of the renormalized 4- and 2-point functions will be obvious.

These identities are not valid for each seperate 4-point-diagram but, of course, just for those groups of graphs which are linked to the same 2-point-function when interpreting one incoming together with one outgoing line as an insertion.

The Ward Identity in the case treated here was already written down in Chapter 6, but for convenience will be stated here again:

$$(a-b) < [\bar{\phi}\phi]_{ab}\phi_{\nu a}\bar{\phi}_{b\nu} >_c = < \phi_{\nu b}\bar{\phi}_{b\nu} >_c - < \bar{\phi}_{a\nu}\phi_{\nu a} >_c \tag{7.1}$$

7.1 One-loop-calculation

In the one-loop-case there is just one diagram that has to be taken care of at the 4-point-level, as well as in the 2-point one. To apply the Ward Identity we will interpret the in- and outgoing line at one vertex as an insertion. The index “b” in the 4-point-graph which is not there anymore plays no role in the calculation of the amplitude as it propagates without “feeling” the loop. Thus we don't loose any information when ignoring it in this calculation. The Identity can be seen in Figure 7.1. It is given by:

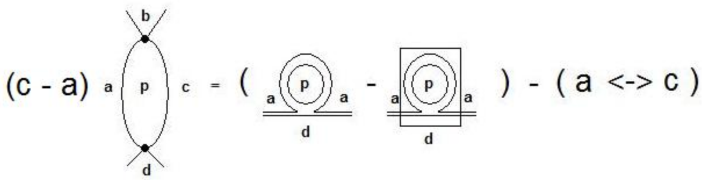

Figure 7.1: 1-loop Ward Identity

$$(c-a)\sum_p \frac{1}{(A+p+a)(A+p+c)} = \sum_p \Big\{ (\frac{1}{A+p+a} - \frac{1}{A+p}) - (a \leftrightarrow c) \Big\} =$$
$$= \sum_p \Big\{ \frac{-a}{(A+p+a)(A+p)} - \frac{-c}{(A+p+c)(A+p)} \Big\} =$$
$$= \sum_p \frac{c-a}{(A+p+a)(A+p+c)}$$
$$\rightarrow \quad \sum_p \frac{1}{(A+p+a)(A+p+c)} = \sum_p \frac{1}{(A+p+a)(A+p+c)} \tag{7.2}$$

So the 1-loop-identity is even exactly valid. Setting the external indices to zero gives the 1-loop-coefficient a' of the 4-point-function $\Gamma^4(0,0,0,0)$ which is needed to compute the boundedness of the β-function.

$$a = c = 0 \qquad \rightarrow \qquad a' = \sum_p \frac{1}{(A+p)^2} \tag{7.3}$$

7.2 Two-loop-calculation

At 2-loop-order we have to treat three different groups of graphs. One corresponding to the TEXTup, one to the TINTup and one to the "Sunshine" graph.

7.2.1 Ward Identity corresponding to the TEXTup graph

Starting with the TEXTup 2-point-diagram we find that there are two corresponding 4-point-graphs depicted in figure 7.2. Therefore

$$(c-a)\sum_{p,q} \Big\{ \frac{1}{(A+p+a)(A+p+c)(A+q+a)(A+q+c)} +$$
$$+ (\frac{1}{(A+p+a)^2(A+p+c)(A+q+a)} - \frac{1}{(A+p+a)^2(A+p+c)(A+q)}) +$$
$$+ (\frac{1}{(A+p+c)^2(A+p+a)(A+q+c)} - \frac{1}{(A+p+c)^2(A+p+a)(A+q)}) \Big\} =$$
$$= \sum_{p,q} \Big\{ (\frac{1}{(A+p+a)^2(A+q+a)} - \frac{1}{(A+p+a)^2(A+q)}) + (a \leftrightarrow c) \Big\}$$

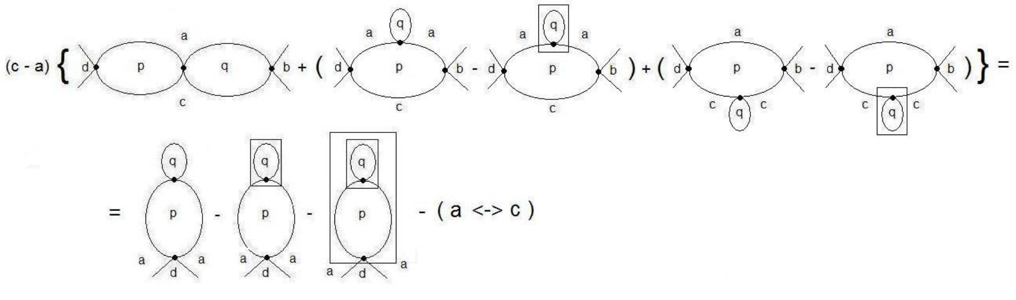

Figure 7.2: 2-Loop Ward Identity for the TEXTup graph

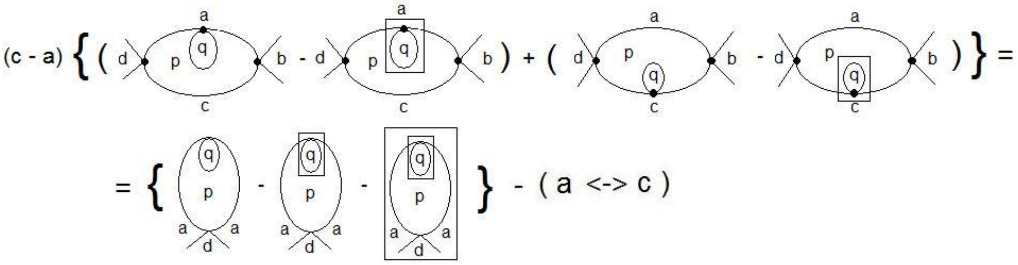

Figure 7.3: 2-Loop Ward Identity for the TINTup graph

Writing all terms of each side on one fraction, one recognizes that the factor $(c-a)$ can be canceled.

$$
\begin{aligned}
&(c-a)\sum_{p,q}\Big\{\frac{(A+p+a)(A+p+c)(A+q)-a(A+p+c)(A+q+c)}{(A+p+a)^2(A+p+c)^2(A+q+a)(A+q+c)(A+q)}-\\
&\quad-\frac{c(A+p+a)(A+q+a)}{(A+p+a)^2(A+p+c)^2(A+q+a)(A+q+c)(A+q)}\\
&=-(c-a)\sum_{p,q}\Big\{\frac{-A^3+a^2c-p^2q-A^2(2p+q)}{(A+p+a)^2(A+p+c)^2(A+q+a)(A+q+c)(A+q)}+\\
&\quad+\frac{ac(c+2p+q)+A(3ac-p(p+2q))}{(A+p+a)^2(A+p+c)^2(A+q+a)(A+q+c)(A+q)}\Big\}
\end{aligned}
\tag{7.4}
$$

The terms on both side cancel exactly, without leaving finite terms, as in the 1-loop case. Setting the external indices to zero one finds that both sides give

$$
\sum_{p,q}\frac{(A+p)^2(A+q)}{(A+p)^4(A+q)^3}=\sum_{p,q}\frac{1}{(A+p)^2(A+q)^2}
\tag{7.5}
$$

which is the contribution of these diagrams to the second order co-efficient "b'" of $\Gamma^4(0,0,0,0)$.

7.2.2 Ward Identity corresponding to the TINTup graph

The next Ward Identity being calculated is the one proportional to the TINTup graph, illustrated in figure 7.3.

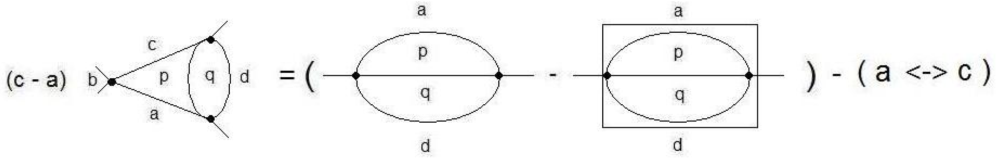

Figure 7.4: 2-Loop Ward Identity for the S graph

$$
\begin{aligned}
(c-a)\sum_{p,q}\Big\{\Big(&\frac{1}{(A+p+a)^2(A+p+c)(A+p+q)}-\\
&-\frac{1}{(A+p+a)^2(A+p+c)(A+q)}\Big)+\\
&+\Big(\frac{1}{(A+p+a)(A+p+c)^2(A+p+q)}-\\
&-\frac{1}{(A+p+a)(A+p+c)^2(A+q)}\Big)\Big\}=\\
=\sum_{p,q}\Big\{&\frac{1}{(A+p+a)^2(A+p+q)}-\frac{1}{(A+p+a)^2(A+q)}-\\
&-\frac{1}{(A+p)^2(A+p+q)}+\frac{1}{(A+p)^2(A+q)}\Big\}
\end{aligned}
$$

$$
\begin{aligned}
\rightarrow\quad &(c-a)\sum_{p,q}\frac{-p(A+p+c)-p(A+p+a)}{(A+p+a)^2(A+p+c)^2(A+p+q)(A+q)}=\\
&=(c-a)\sum_{p,q}\frac{-p(A+p)^2(2A+2p+a+c)}{(A+p+a)^2(A+p+c)^2(A+p)^2(A+p+q)(A+q)}
\end{aligned}
\tag{7.6}
$$

The two sides of this identity cancel to zero too. Again, setting the external indices to zero the contribution to $\Gamma^4(0,0,0,0)$ is received.

$$
\begin{aligned}
&\sum_{p,q}\frac{-2p(A+p)}{(A+p)^4(A+p+q)(A+q)}=\sum_{p,q}\frac{-2p}{(A+p)^3(A+p+q)(A+q)}=\\
&=\sum_{p,q}\Big(\frac{2}{(A+p)^3(A+p+q)}-\frac{2}{(A+p)^3(A+q)}\Big)
\end{aligned}
\tag{7.7}
$$

7.2.3 Ward Identity corresponding to the S graph

The last Identity which has to be taken into account is seen in Figure 7.4.

$$
\begin{aligned}
&(c-a)\sum_{p,q}\frac{1}{(A+p+a)(A+p+c)(A+p+q)(A+q+d)}=\\
&=\sum_{p,q}\Big\{\Big(\frac{1}{(A+p+a)(A+p+q)(A+q+d)}-\frac{1}{(A+p)(A+p+q)(A+q)}\Big)-\\
&\qquad-(a\leftrightarrow c)\Big\}
\end{aligned}
$$

$$\rightarrow \quad (c-a)\sum_{p,q}\frac{1}{(A+p+a)(A+p+c)(A+p+q)(A+q+d)} =$$

$$= (c-a)\sum_{p,q}\frac{(A+p)(A+q)}{(A+p+a)(A+p+c)(A+p)(A+p+q)(A+q+d)(A+q)} \tag{7.8}$$

The difference of these terms is zero as well and therefore the Ward Identity is, at least up to 2-loop-order, not just correct up to irrelevant terms but an exact identity. Like the tadpole graph, the diagram “E” has two different orientations, the one shown in figure 7.4, and the one where the “Eye” looks in the opposite direction. This gives a Ward Identity where the index “b” and “d” are exchanged. Putting the external indices to zero, there is no difference between them anymore and we find that their contribution to the coefficient of Γ^4 is

$$a=c=d=0 \qquad \rightarrow \qquad \sum_{p,q}\frac{2}{(A+p)^2(A+p+q)(A+q)} \tag{7.9}$$

Now the 4-point-function obtained by the Ward Identities can be written down:

$$\begin{aligned}\Gamma^4(0,0,0,0) = 1 - a'\tilde{\lambda} + b'\tilde{\lambda}^2 = 1 - \frac{\tilde{\lambda}}{2}\sum_{p}\frac{1}{(A+p)^2} +& \\ +\frac{\tilde{\lambda}^2}{8}\sum_{p,q}\Big\{&\frac{2}{(A+p)^3(A+p+q)} - \frac{2}{(A+p)^3(A+q)} + \\ &+\frac{2}{(A+p)^2(A+p+q)(A+q)} + \frac{1}{(A+p)^2(A+q)^2}\Big\}\end{aligned} \tag{7.10}$$

Comparing with the result of section 4, we see that it is identical and hence gives the correct result for the boundedness of the β-function.

Chapter 8

Grosse-Wulkenhaar-model in a magnetic field

The methods of the general proof of the Grosse-Wulkenhaar-model up to all orders by Rivasseau et al. were later used to proof the vanishing of the β-function up to all orders of the GW model in a magnetic field (see [13]). In this proof they use the complex model and add an extra term with an external magnetic field. This is a generalization of the Langmann-Szabo-Zarembo model which is the general noncommutative $\phi_4^{\star 4}$-model in a magnetic field without the harmonic potential term. This model is especially interesting for being a toy model of the quantum Hall effect.

The proof again constructs the Ward Identities and uses the result the calculate the Dyson-Schwinger-equation.

The GW-model in an external magnetic field is given by

$$\begin{aligned} S[\phi] = \int \mathrm{d}^4x \Big\{ & \partial_\mu\bar{\phi}) \star (\partial^\mu \phi) + \Omega(\tilde{x}_\mu \bar{\phi}) \star (\tilde{x}^\mu \phi) - 2iB\bar{\phi}(\tilde{x}_\mu \partial^\mu)\phi + \\ & + \mu(\bar{\phi} \star \phi) + \frac{\lambda}{2}\bar{\phi} \star \phi \star \bar{\phi} \star \phi) \Big\} \end{aligned} \tag{8.1}$$

where B is the magnetic field, μ stands for the mass, $\tilde{x}_\mu = 2(\theta^{-1}_{\mu\nu})x_\nu$ and $(\Omega - B^2)$ is a harmonic potential. The standard GW-model is recovered in the limit $B \to 0$.

The proof starts again by constructing the generating functional of the model

$$\begin{aligned} & Z(\eta, \bar{\eta}) = \int \mathrm{d}\phi \mathrm{d}\bar{\phi} e^{-S(\phi,\bar{\phi}) + F(\eta,\bar{\eta},\phi,\bar{\phi})} \\ & F(\eta, \bar{\eta}, \phi, \bar{\phi}) = \bar{\phi}\eta + \bar{\eta}\phi \\ & S(\phi, \bar{\phi}) = \bar{\phi}X_L\phi + \phi X_R\bar{\phi} + A\bar{\phi}\phi + \frac{\lambda}{2}\phi\bar{\phi}\phi\bar{\phi} \\ & \phi = (\phi_{mn}) \qquad X_L = qm\delta_{mn} \qquad X_R = pm\delta_{mn} \qquad q = 1 + B \qquad p = 1 - B \end{aligned} \tag{8.2}$$

with some modifications with respect to the general model to include the external field into the definitions. Here, the mass parameter μ is rescaled and now given as $A = 2 + \frac{\mu^2\theta}{4}$ and the kinetic part together with the harmonic potential including the magnetic field is included in the matrix operators X_L and X_R with unequal weights q and p. As the harmonic potential should be bounded, because of the Langmann-Szabo-symmetry, between 0 and 1 we need $0 < B \leq \Omega$ to have a stable model. It can be seen as a deformed matrix theory with dual parameters q and p. In the limit $q \to 1$ and $p \to 1$ which means $B \to 0$ the GW-model is recovered.

The propagator of the GW-model and its variables have to adjusted to include the deformation parameters p and q:

$$C_{mn;kl} = C_{mn}\delta_{ml}\delta_{nk} \qquad C_{mn} = \frac{1}{A + qm + pn} \tag{8.3}$$

where $m, n \in \mathbb{N}^2$. As the complex model is used the propagators are again oriented and it is distinguished between acting on the "left" or on the "right" index (for a more detailed description see section 6). To proof the boundedness of the beta-function we need the amputated, 1PI 4-point-function $\Gamma^4(m, n, k, l)$, and the corresponding wave-function-renormalization, which is given as the derivation of the self energy $\Sigma(m, n)$, which is the amputated, 1PI 2-point-function, with respect to on of the external indices. Further the wave-function-renormalization needs to take the parameters p and q into account, and therefore has to distinguish between the left and the right side of the ribbon graph:

$$Z_L = 1 - \frac{1}{q}\partial_L\Sigma(0,0) \qquad Z_R = 1 - \frac{1}{p}\partial_R\Sigma(0,0) \tag{8.4}$$

The complete wave-function-renormalization is then given by $Z = \sqrt{Z_L Z_R}$ and the renormalization of the general GW-model is recovered when q and p are taken to 1 and the "left" and the "right" wave-function-renormalization become equal. Thus we find

$$\lambda_{eff} = \frac{\Gamma^4(0,0,0,0)}{\sqrt{Z_L Z_R}} \tag{8.5}$$

and can write down the reformulated theorem valid for the modified model:

Boundedness of β-function in a magnetic field 1

$$\Gamma^4(0,0,0,0) = \lambda(1 - \frac{1}{q}\partial_L\Sigma(0,0))(1 - \frac{1}{p}\partial_R\Sigma(0,0)) \tag{8.6}$$

where λ is the bare coupling constant. Like above it can be understood as a bare coupling, reexpressed as a series in the renormalized one as well to be valid for the renormalized equation.

8.1 Ward Identities

First the Ward-Identities related to the U(N)-symmetry have to be constructed. This is done in exactly the same way as in the proof of the general GW-model done in the last section. Of course, one now has to differentiate between the "left" and "right" variation because of the unequal weights p and q. But in the actual calculation the only difference comes from using the explicit form of the matrix operators X_L and X_R and putting their constants in front of the correlation functions (see (6.7)). Here, the factor $(a-b)$ changes because of the deformation parameters and becomes $q(a-b)$ for the "left" variation and $-p(a-b)$ for the "right" one. The negative sign cancels with the sign coming from the "right" variation itself. Thus, finally we find the following expressions for the 2-pt, and

4-pt-Ward-Identities:

$$\begin{aligned} q(a-b) &< [\bar\phi\phi]_{ab}\phi_{\nu a}\bar\phi_{b\nu} >_c = < \phi_{\nu b}\bar\phi_{b\nu} >_c - < \bar\phi_{a\nu}\phi_{\nu a} >_c \\ p(a-b) &< [\bar\phi\phi]_{ab}\phi_{\nu a}\bar\phi_{b\nu} >_c = < \phi_{\nu b}\bar\phi_{b\nu} >_c - < \bar\phi_{a\nu}\phi_{\nu a} >_c \end{aligned} \tag{8.7}$$

$$\begin{aligned} q(a-b) &< \phi_{\alpha a}[\bar\phi\phi]_{ab}\bar\phi_{b\nu}\phi_{\nu\delta}\bar\phi_{\delta\alpha} >_c = < \phi_{\alpha b}\bar\phi_{b\nu}\phi_{\nu\delta}\bar\phi_{\delta\alpha} >_c - < \phi_{\alpha a}\bar\phi_{a\nu}\phi_{\nu\delta}\bar\phi_{\delta\alpha} >_c \\ p(a-b) &< \phi_{\alpha a}[\bar\phi\phi]_{ab}\bar\phi_{b\nu}\phi_{\nu\delta}\bar\phi_{\delta\alpha} >_c = < \phi_{\alpha b}\bar\phi_{b\nu}\phi_{\nu\delta}\bar\phi_{\delta\alpha} >_c - < \phi_{\alpha a}\bar\phi_{a\nu}\phi_{\nu\delta}\bar\phi_{\delta\alpha} >_c \end{aligned} \tag{8.8}$$

8.2 Proofing the theorem

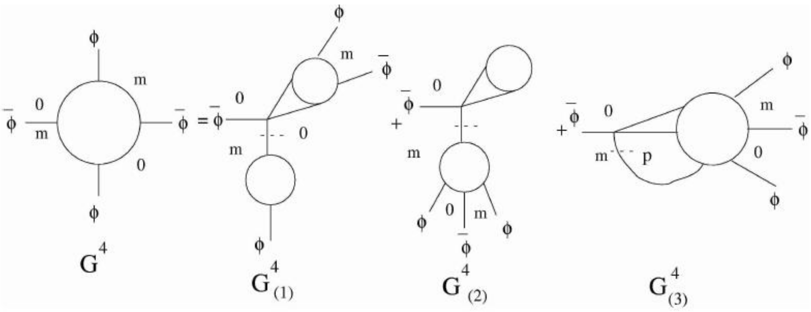

Figure 8.1: The left Dyson-Schwinger-Equation

Analogous to the proof for the general model, we start by constructing the Dyson-Schwinger-equations for the left and the right variation respectively which makes a difference now because of the wave-function-renormalization. The steps are equal however and the proof will be just given for the left variation. The “right” results will be written down at the end of this section.

The proof can be done in the bare and the mass-renormalized theory respectively with the differences already explained in the section 6. The proof here will be done in the mass-renormalized case.

The G^4_2-graph is zero after mass renormalization and therefore the relevant “generalized” Feynman graphs are G^4_1 and G^4_3.

Let the function $G^2(m,n)$ be the connected, planar, one broken face 2-point-function given by

$$G^2(m,n) = \frac{1}{C^{-1}_{mn} - \Sigma(m,n)} = \frac{1}{A + qm - \Sigma(m,n)} \tag{8.9}$$

and the 2-point-function with one left insertion, according to the Ward Identities

$$q(a-b)G^{2,L}_{ins}(a,b,\nu) = G^2(b,\nu) - G^2(a,\nu). \tag{8.10}$$

So the first graph in the left Dyson-Schwinger-equation can be written as:

$$G^4_{(1)}(0,m,0,m) = -\lambda C_{0m} G^2(0,m) G^{2,L}_{ins}(0,0;m) \tag{8.11}$$

Using the Ward Identity in Equation (8.10), we can write

$$\begin{aligned} G^{2,L}_{ins}(0,0;m) &= \lim_{\xi\to 0} G^{2,L}_{ins}(\xi,0;m) = \frac{1}{q}\lim_{\xi\to 0}\frac{G^2(0,m)-G^2(\xi,m)}{\xi} = \\ &= -\frac{1}{q}\partial_L G^2(0,m) \end{aligned} \tag{8.12}$$

Applying the derivation on the definition of $G^2(0,m)$ in (8.9) we get

$$-\frac{1}{q}\partial_L G^2(0,m) = \frac{1}{q}\frac{1}{(C_{0m}^{-1}-\Sigma(0,m))^2}(q-\partial_L\Sigma(0,m)) \tag{8.13}$$

Inserting all definitions into (8.11) we can rewrite it as

$$\begin{aligned} G^4_{(1)}(0,m,0,m) &= \frac{\lambda}{q}C_{0m}\frac{C_{0m}C_{0m}^2(q-\partial_L\Sigma(0,m))}{(1-C_{0m}\Sigma(0,m))(1-C_{0m}\Sigma(0,m))^2} = \\ &= \lambda(G^2(0,m))^4\frac{C_{0m}}{G^2(0,m)}(1-\partial_L\Sigma(0,m)) \end{aligned} \tag{8.14}$$

Taylor expanding the self-energy up to first order, and therefore up to irrelevant terms we find

$$\Sigma(n,m) = \Sigma(0,0) + n\partial_L\Sigma(n,m)|_{m=n=0} + m\partial_R\Sigma(n,m)|_{m=n=0} \tag{8.15}$$

and $G^2(0,m)$ can be expressed as

$$G^2(0,m) = \frac{1}{pm + A_{bare} - \Sigma 0, m} = \frac{1}{m(p-\partial_R\Sigma(0,0)) + A_{ren}}. \tag{8.16}$$

Hence,

$$\begin{aligned} \frac{C_{0m}}{G^2(0,m)} &= \frac{m(p-\partial_R\Sigma(0,0)) + A^R}{pm + A^R} = \\ &= \frac{(m + A^R/p)(1-\partial_R\Sigma(0,0) + A^R - A^R + A^R/p\partial_R\Sigma(0,0)}{pm + A^R} = \\ &= \frac{1}{p}(p-\partial_R\Sigma(0,0)) + \frac{A^R}{p(pm+A^R)}\partial_R\Sigma(0,0) \end{aligned} \tag{8.17}$$

and finally

$$\begin{aligned} G^4_{(1)}(0,m,0,m) = -\lambda(G^2(0,m))^4\Big(\frac{1}{p}(p-\partial_R\Sigma(0,0)) + \frac{A^R}{p(pm+A^R)}\partial_R\Sigma(0,0)\Big) \\ \frac{1}{q}(q-\partial_L\Sigma(0,m)). \end{aligned} \tag{8.18}$$

Now we have to care about diagram $G^4_{(3)}$ to put it in a useful form. When cutting the line “to the right” at the first vertex, namely the one belonging to the face p, one can decompose the bare graph into

$$G^{4,bare}_{(3)} = -\lambda C_{0m}\sum_p G^{4,bare,L}_{ins}(0,p;m,0,m) \tag{8.19}$$

As already argued in the last section, the face which was opened to be able to define the insertion, could have belonged to a diverging loop and thus have a counterterm. Calculating in the renormalized theory, this fact has to be taken care of and this, otherwise lost, counterterm added to the equation.

$$G^4_{(3)} = -\lambda C_{0m} \sum_p G^{4,L}_{ins}(0,p;m,0,m) - C_{0m}(CT^L_{lost})G^4(0,m,0,m) \tag{8.20}$$

As the counterterms which have just a face on the "left" side of the propagator do not get lost when cutting the line, the self-energy can be seperated into a part with a contribution to the "right" face and the generalized "left" tadpole for the rest:

$$\Sigma(m,n) = T^L(m,n) + \Sigma^R(m,n) \tag{8.21}$$

With this identity we can rewrite the lost counterterm as

$$CT_{lost} = \Sigma^R(0,0) = \Sigma(0,0) - T^L \tag{8.22}$$

Now we want to compute the "right" contribution to the self-energy.

$$\begin{aligned} \Sigma^R(0,0) &= -\frac{\lambda}{G^2(0,0)} \sum_p G^2_{ins}(0,p;0) = -\frac{\lambda}{q}\frac{1}{G^2(0,0)} \sum_p \frac{1}{p}(G^2(0,0) - G^2(p,0)) = \\ &= -\frac{\lambda}{q} \sum_p \frac{1}{p}\Big(1 - \frac{G^2(p,0)}{G^2(0,0)}\Big) \end{aligned} \tag{8.23}$$

Then, equation (8.20) togehter with (8.23) is

$$\begin{aligned} G^4_{(3)}(0,m,0,m) = -\lambda C_{0m} \sum_p G^{4,L}_{ins}(0,p;m,0,m) - \\ - \frac{(-\lambda)}{q} C_{0m} G^4(0,m,0,m) \sum_p \frac{1}{p}\Big(1 - \frac{G^2(p,0)}{G^2(0,0)}\Big) \end{aligned} \tag{8.24}$$

Again we rewrite the insertion using the Ward Identity:

$$-\lambda C_{0m} \sum_p G^{4,L}_{ins}(0,p;m,0,m) = -\frac{\lambda}{q} C_{0m} \sum_p \frac{1}{p}(G^4(0,m,0,m) - G^4(p,m,0,m)) \tag{8.25}$$

The second term can be neglected because its denominator is at least of power 3 and therefore irrelevant. Now we can rewrite $G^4_{(3)}$ as

$$G^4_{(3)} = -\frac{\lambda}{q} C_{0m} \frac{G^4(0,m,0,m)}{G^2(0,0)} \sum_p \frac{G^2(p,0)}{p} \tag{8.26}$$

The last step to obtain a useful expression for this graph we have to reformulate the sum over p in the last equation.

$$\sum_p \frac{G^2(p,0)}{p} = \sum_p \frac{G^2(p,0)}{p} \Big(\frac{1}{G^2(0,1)} - \frac{1}{G^2(0,0)}\Big) \frac{1}{p - \partial_R \Sigma(0,0)} \tag{8.27}$$

Repeating the steps from equation (8.23) we find that

$$\Sigma^R(0,1) = -\frac{\lambda}{q} \sum_p \frac{1}{p}\Big(1 - \frac{G^2(p,1)}{G^2(0,1)}\Big) = -\frac{\lambda}{q} \sum_p \frac{1}{p}\Big(1 - \frac{G^2(p,0)}{G^2(0,1)}\Big) \tag{8.28}$$

Substituting the expressions for $\Sigma(0,0)^R$ and $\Sigma^R(0,1)$ into the identity for the sum over p we find

$$-\lambda\sum_p \frac{G^2(p,0)}{p} = \frac{q(\Sigma^R(0,0)-\Sigma^R(0,1))}{p-\partial_R\Sigma(0,0)} = -\frac{q\partial_R\Sigma^R(0,0)}{p-\partial_R\Sigma(0,0)} \tag{8.29}$$

and $G^4_{(3)}$ adds up to

$$\begin{aligned} G^4_{(3)}(0,m,0,m) &= -C_{0m}G^4(0,m,0,m)\frac{1}{G^2(0,0)}\frac{q\partial_R\Sigma^R(0,0)}{p-\partial_R\Sigma(0,0)} = \\ &= -G^4(0,m,0,m)\frac{A^R\partial_R\Sigma^R(0,0)}{(pm+A^R)(q\partial_R\Sigma^R(0,0))} \end{aligned} \tag{8.30}$$

Writing down the resulting Dyson-Schwinger-equation we have

$$\begin{aligned} &G^4(0,m,0,m)\Big(1+\frac{A^R\partial_R\Sigma^R(0,0)}{(pm+A^R)(q\partial_R\Sigma^R(0,0))}\Big) = \\ &\lambda_{bare}(G^2(0,m))^4\Big(\frac{1}{p}(p-\partial_R\Sigma(0,0)) + \frac{A^R}{p(pm+A^R}\partial_R\Sigma(0,0)\Big)\frac{1}{q}(q-\partial_L\Sigma(0,m)) \end{aligned} \tag{8.31}$$

Multiplying the equation by $(p-\partial_R\Sigma^R(0,0))/p$, and amputating four times one finally finds the theorem to proof:

$$\Gamma^4(0,0,0,0) = \lambda(1-\frac{1}{q}\partial_L\Sigma(0,0))(1-\frac{1}{p}\partial_R\Sigma(0,0)) \tag{8.32}$$

Chapter 9

Final Remarks

The reason to search for a Quantum Field theory which maybe could one day include gravity, on non-commutative spaces, was the observation that gravity changes the geometry of the space in which the Field theory is defined. Alain Connes, Ali Chamseddine and others found out that the classical standard model emerges very natural out of a non-commutative space. The hope to be able to define a more general theory on such a space is therefore quite natural.

Showing the renormalizablity of the Grosse-Wulkenhaar-model was the first step in this direction as renormalizable theories play a central part in describing real physics, as can be argued by using the renormalization group approach. There, renormalizable theories are those which survive the RG flow which means that those theories really have affects on physics at the corresponding scales.

The proof of the boundendness of the β-function showed that there is no more Landau ghost in this non-commutative model and that it is not asymptotically free but just bounded. This is furthermore a step to describe the model in a non-perturbative setting without using cut-offs. The boundedness makes it the only yet known just-renormalizable model with quadratic divergences which has this property and an interesting starting point for the search of a non-commutative standard model.

Besides this application to high energy physics, related models as the Langmann-Szabo-Zarembo model indicate the possible usefullness of non-commutative models in describing for instance the Quantum Hall effect.

The achivements made with the Grosse-Wulkenhaar model are very encouraging but still there is a lot of work to be done. A first possible proof of the renormalizability of a non-commutative U(1)-gauge theory [14] may already be the next step and definitely shows that the fascination of the possiblities found on non-commutative spaces is growing rapidly.

Chapter 10

Appendix

10.1 Two-Loop-Calculation

To solve some of the integrals the following dilogarithm identities are needed to map the dilogarithm into its convergent interval between 0 and 1:

$$Li_2[z] = -Li_2[\frac{1}{z}] - \frac{1}{2}(\ln[-z])^2 - \frac{\pi^2}{6} \qquad \text{for z} \notin (0,1) \tag{10.1}$$

$$Li_2[z] = -Li_2[1-z] - \ln[z]\ln[1-z] + \frac{\pi^2}{6} \qquad \text{Euler identity} \tag{10.2}$$

Before the actual two-loop-diagrams are calculated, some useful integrals are calculated below.

$$\begin{aligned}
\int_0^\Lambda\!\!\int_0^\Lambda \frac{\mathrm{d}p_1\mathrm{d}p_2}{A+p_1+p_2} &= \int_0^\Lambda \mathrm{d}p_2\Big(\ln[A+\Lambda+p_2]-\ln[A+p_2]\Big) = \\
&= (A+2\Lambda)\Big(\ln[A+2\Lambda]-1\Big) - 2(A+\Lambda)\Big(\ln[A+\Lambda]-1\Big) + A\Big(\ln[A]-1\Big) = \\
&= (A+2\Lambda)\ln[2\Lambda] + (A+2\Lambda)\ln[1+\frac{A}{2\Lambda}] - 2(A+\Lambda)\ln[\Lambda] - \\
&\quad - 2(A+\Lambda)\ln[1+\frac{A}{\Lambda}] + A\ln[A] = \\
&\overset{\Lambda\to\infty}{=} 2\ln[2]\Lambda - A\ln[\Lambda] + A\ln[2A]
\end{aligned}$$

$$\begin{aligned}
\int_0^\Lambda\!\!\int_0^\Lambda \frac{\mathrm{d}p_1\mathrm{d}p_2}{(A+p_1+p_2)^2} &= \int_0^\Lambda \mathrm{d}p_2\Big(\frac{-1}{(A+\Lambda+p_2)}+\frac{1}{(A+p_2)}\Big) = \\
&= -\ln[A+2\Lambda] + 2\ln[A+\Lambda] - \ln[A] = \\
&= -\ln[2\Lambda] - \ln[1+\frac{A}{2\Lambda}] + 2\ln[\Lambda] + 2\ln[1+\frac{A}{\Lambda}] - \ln[A] = \\
&\overset{\Lambda\to\infty}{=} \ln[\Lambda] - \ln[2A]
\end{aligned}$$

$$\int\limits_0^\Lambda\int\limits_0^\Lambda \frac{\mathrm{d}p_1\mathrm{d}p_2}{(A+p_1+p_2)^3} = \int\limits_0^\Lambda \mathrm{d}p_2\Big(-\frac{1}{2(A+\Lambda+p_2)^2}+\frac{1}{2(A+p_2)}\Big) =$$
$$= \frac{1}{2(A+2\Lambda)} - \frac{1}{A+\Lambda} + \frac{1}{2A} =$$
$$\overset{\Lambda\to\infty}{=} \frac{1}{2A}$$

10.1.1 TEXTup

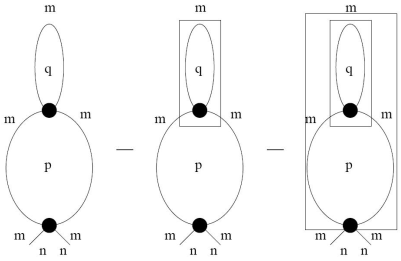

Figure 10.1: Renormalizing the "TEXTup"-graph

The renormalized amplitude for the TEXTup graph is given by

$$\begin{aligned} G_{mn}^{TEXT_{up},R} &= \int\limits_0^\Lambda\int\limits_0^\Lambda \mathrm{d}^2p\mathrm{d}^2q\Big\{\frac{1}{(A+p+m)^2(A+q+m)} - \\ &- \frac{1}{(A+p+m)^2(A+q)} - \Big(\frac{1}{(A+p)^2(A+q)} - \\ &- \frac{1}{(A+p)^2(A+q)}\Big)\Big\} \end{aligned} \tag{10.3}$$

and represented as Feynman graphs which can be seen in figure 10.1. First the diverging part will be calculated:

$$\begin{aligned} &\int\limits_0^\Lambda\int\limits_0^\Lambda \mathrm{d}^2p\mathrm{d}^2q\frac{1}{(A+p+m)^2(A+q+m)} = \\ &\overset{\Lambda\to\infty}{=} \Big(2\ln[2]\Lambda - (A+m)\ln[\Lambda] + (A+m)\ln[2(A+m)]\Big) \\ &\qquad \Big(\ln[\Lambda] - \ln[2(A+m)]\Big) = \\ &= \Lambda\Big(2\ln[2]\ln[\Lambda] - 2\ln[2]\ln[m+A] - 2(\ln[2])^2\Big) - (A+m)\ln[\Lambda]^2 + \\ &\qquad + \ln[\Lambda]\Big(2(A+m)\ln[2] + 2(A+m)\ln[m+A]\Big) - \\ &\qquad - (A+m)\ln[2]^2 - 2(A+m)\ln[2]\ln[m+A] - (A+m)\ln[m+A]^2 \end{aligned}$$

The only relevant counterterm is the subdivergence because the overall divergent terms cancel each other. The subdivergence corresponds to the divergence of the tadpole and this just means to exchange $\frac{1}{A+q+a}$ with $\frac{1}{A+q}$. The renormalized amplitude is now

$$\begin{aligned} G^{TEXT_{up},R}_{mn} = & -m\ln[\Lambda]^2 + \ln[\Lambda]\Big(-A\ln[A] + A\ln[m+A] + 2m\ln[2]+ \\ & + 2m\ln[m+A]\Big) - m\ln[2]^2 + A\ln[2]\ln[A] - 2m\ln[2]\ln[m+A]- \\ & - A\ln[2]\ln[m+A] + A\ln[A]\ln[m+A]- \\ & - m\ln[m+A]^2 - A\ln[m+A]^2 \end{aligned} \tag{10.4}$$

The contribution to the field-strength renormalization is obtained by differentiating once wth respect to the external momentum:

$$\begin{aligned} -\partial_{m_1} G^{TEXT_{up},R}_{mn}\Big|_{m=n=0} &= \sum_{p,q} \frac{1}{(A+p)^2(A+q)^2} = \\ &= (\ln[\Lambda] - \ln[2] - \ln[A])^2 \end{aligned} \tag{10.5}$$

10.1.2 TINTup

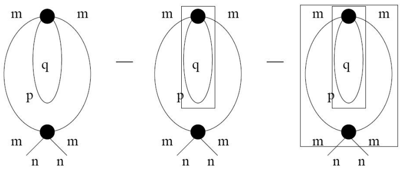

Figure 10.2: Renormalizing the "TINTup"-graph

Next the TINTup graph will be renormalized. Here again, we have to subtract the subdivergence before we add the overall counterterm (see Figure 10.2). The amplitude for the graph is given by

$$\begin{aligned} G^{TINT_{up},R}_{mn} = & \int\limits_0^\Lambda\!\!\int\limits_0^\Lambda \mathrm{d}^2p\mathrm{d}^2q \Big\{ \frac{1}{(A+p+m)^2(A+p+q)} - \\ & - \frac{1}{(A+p+m)^2(A+q)} - \Big(\frac{1}{(A+p)^2(A+p+q)} - \\ & - \frac{1}{(A+p)^2(A+q)}\Big)\Big\} \end{aligned} \tag{10.6}$$

The divergent integral is best solved by evaluating first the integration by d^2q:

$$\int\limits_0^\Lambda\!\!\int\limits_0^\Lambda \frac{\mathrm{d}q^2}{A+q+p} \overset{\Lambda\to\infty}{=} 2\ln[2]\Lambda - (A+p)\ln[\Lambda] + (A+p)\ln[2] + (A+p)\ln[A+p]$$

Now, the various parts are integrated, together with the $\frac{1}{(A+p+m)^2}$-factor, separately.

$$\int\limits_0^\Lambda\!\!\int\limits_0^\Lambda \mathrm{d}^2p \frac{2\ln[2]\Lambda}{(A+p+m)^2}$$

$$
\begin{aligned}
(\ln[2]-\ln[\Lambda])\int\limits_0^\Lambda\!\!\int\limits_0^\Lambda \mathrm{d}^2p\frac{A+p}{(A+p+m)^2} &= \text{add and subtract m} = \\
&= (\ln[2]-\ln[\Lambda])\int\limits_0^\Lambda\!\!\int\limits_0^\Lambda \mathrm{d}^2p\Big(\frac{1}{(A+p+m)}-\frac{m}{(A+p+m)^2}\Big)
\end{aligned}
$$

$$
\begin{aligned}
&\int\limits_0^\Lambda\!\!\int\limits_0^\Lambda \mathrm{d}^2p\frac{(A+p+m-m)\ln[A+p]}{(A+p+m)^2} = \\
&\quad\int\limits_0^\Lambda\!\!\int\limits_0^\Lambda \mathrm{d}^2p\Big(\frac{\ln[A+p]}{(A+p+m)}-\frac{m\ln[A+p]}{(A+p+m)^2}\Big)
\end{aligned}
$$

Finally, the divergent graph TINTup is given by:

$$
\begin{aligned}
G_{mn}^{TINT_{up}} = {} & \Lambda(2\ln[2]\ln[\Lambda]-2\ln[2]+\ln[2]^2-2\ln[2]\ln[A+m])+\ln[\Lambda]^2(\frac{A}{2}+m)+ \\
& +\ln[\Lambda](A-m-A\ln[2]-2m\ln[2]-A\ln[A+m]-2m\ln[A+m])- \\
& -m-A\ln[2]+m\ln[2]+\frac{3A}{2}\ln[2]^2+3m\ln[2]^2-2A\ln[A] \\
& +A\ln[A+m]+m\ln[A+m]+A\ln[2]\ln[A+m] \\
& +2m\ln[2]\ln[A+m]+\frac{A}{2}(\ln[A+m])^2+ \\
& +m\ln[A+m]^2+ALi_2(\frac{m}{A+m})+2mLi_2(\frac{m}{A+m})
\end{aligned}
$$

The subdivergence is again given by substituting the tadpole graph for the $\frac{1}{A+p+q}$-term. In this case, where the tadpole points into the other loop, the overall divergence is not zero and needs to be subtracted as well. These are the last two terms in the renormalized amplitude. They consist of the first two terms, with the external index m set to zero. Thus the renormalized amplitude is received by adding/subracting the terms from each other.

$$
\begin{aligned}
G_{mn}^{TINT_{up},R} = {} & m(\ln[\Lambda])^2+\ln[\Lambda](-m-2m\ln[2]+2A\ln[A]-2A\ln[A+m]- \\
& -2m\ln[A+m])-m+m\ln[2]+3m(\ln[2])^2-A\ln[A]- \\
& -2A\ln[2]\ln[A]-\frac{3A}{2}(\ln[A])^2+A\ln[A+m]+m\ln[A+m]+ \\
& +2A\ln[2]\ln[A+m]+2m\ln[2]\ln[A+m]+A\ln[A]\ln[A+m]+ \\
& +\frac{A}{2}(\ln[A+m])^2+m(\ln[A+m])^2+ALi_2(-\frac{m}{A+m})+ \\
& +2mLi_2(\frac{m}{A+m})
\end{aligned} \tag{10.7}
$$

The field-strength contribution is

$$
\begin{aligned}
-\partial_{m_1} G_{mn}^{TINT_{up},R}\Big|_{m=n=0} &= \sum_{p,q}\Big(\frac{2}{(A+p)^3(A+p+q)} - \frac{2}{(A+p)^3(A+q)}\Big) = \\
&= -\ln[\Lambda]^2 + \ln[\Lambda](3+2\ln[2]+2\ln[A]) - \\
&- 3\ln[2] - 3\ln[2]^2 - 3\ln[A] - 2\ln[2]\ln[A] - \ln[A]^2 \qquad (10.8)
\end{aligned}
$$

10.1.3 TINTdown and TEXTdown

These two graphs are exactly the same as the TINTup and TEXTup graphs with the external index "m" exchanged for "n".

10.1.4 S

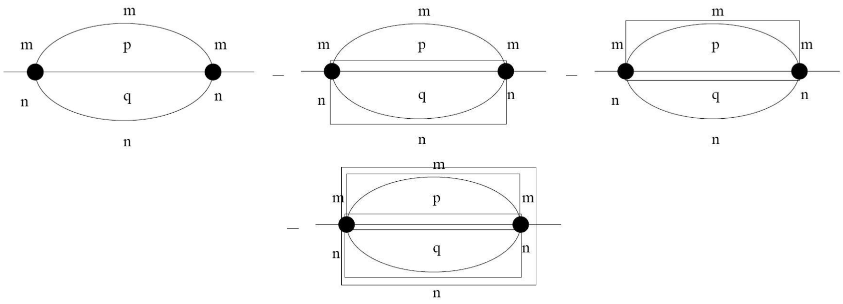

Figure 10.3: Renormalizing the sunrise-graph

The result of the bare graph is already stated in section 4 and the counterterms are easily calculated with the integrals at the beginning of the Appendix. Thus, we find that the final result for the graph "S" is:

$$
\begin{aligned}
G_{mn}^{S,R} = &-\frac{m+n}{2}\ln[\Lambda]^2 + \ln[\Lambda]\Big((m+n)\ln[A] + (m+n)\ln[2]\Big) + \\
&+ \text{finite terms} \qquad (10.9)
\end{aligned}
$$

Finally, the contribution to the field-strenght-renormalization is the following

$$
\begin{aligned}
-\partial_{m_1} G_{mn}^{S,R}\Big|_{m=n=0} &= \sum_{p,q}\Big(\frac{1}{(A+p)^2(A+p+q)(A+q)} - \frac{1}{(A+p)^2(A+q)^2}\Big) = \\
&= \frac{(\ln[\Lambda])^2}{2} - \ln[\Lambda](\ln[2]+\ln[A]) - \\
&- 1 + \frac{3(\ln[2])^2}{2} + \ln[2]\ln[A] + \frac{(\ln[A])^2}{2} \qquad (10.10)
\end{aligned}
$$

Chapter 11

Zusammenfassung

In dieser Arbeit habe ich das Grosse-Wulkenhaar-Modell(GW-Modell) am selbstdualen Punkt studiert. Hierbei handelt es sich um ein nichtkommutatives, skalares Modell, für das als erstes nichtkommutatives Modell die Renormalisierbarkeit gezeigt werden konnte.

$$S[\phi] = \int \mathrm{d}^4x \Big\{ \frac{1}{2}(\partial_\mu \phi) \star (\partial^\mu \phi) + \frac{\Omega^2}{2}(\tilde{x}_\mu \phi) \star (\tilde{x}^\mu \phi) + \frac{m^2}{2}(\phi \star \phi) + \frac{\lambda}{2} \phi \star \phi \star \phi \star \phi) \Big\}$$

Hier steht "m" für die Masse, "λ" für die Kopplungskonstante und "Ω" für die Oszillatorfrequenz. Es erweitert das standard nichtkommutative $\phi^{\star,4}$-Modell um einen Oszillator-Term der das Modell am ausgezeichneten Punkt $\Omega = 1$ invariant unter der Langmann-Szabo-Dualität macht. Dadurch ist eine Unterscheidung zwischen dem Orts- und Impulsraum nicht mehr möglich. Außerdem lässt sich an diesem Punkt das GW-Modell als lokales Matrixmodell darstellen. Das bedeutet dass das Feld ϕ als diagonale Matrix geschrieben werden kann wodurch sich die durchzuführenden Rechnungen wesentlich vereinfachen.

Ich habe in dieser Arbeit die Renormalisierung dieses Modells in zwei und vier Dimensionen jeweils bis zur zweiten Loop-Ordnung für die, nach der Renormalisierungsgruppe, relevanten Feynmangraphen explizit durchgeführt um danach eine weitere faszinierende Eigenschaft dieses Modells, nämlich die Beschränktheit der Beta-Funktion, nach dem Artikel von Rivasseau et al. zu berechnen. Dieser zeigt, dass der Unterschied zwischen der nackten und der renormalisierten Kopplungskonstante des Modells endlich ist und daher die Betafunktion beschränkt. Diese Eigenschaft ist bisweilen für kein anderes Modell bekannt und eröffnet erstmals die Möglichkeit ein quantenfeldtheoretisches Modell konstruktiv, also ohne Divergenzen, darzustellen.

Ich verwende meine aus der Renormalisierung erhaltenen Resultate um diese Eigenschaft für die Kopplungskonstante des Modells bis zur zweiten Ordnung zu zeigen. Danach werden die einzelnen Schritte des Beweises der Beschränktheit in alle Ordnungen detailliert nachvollzogen. Dieser Beweis baut auf den Ward-Identitäten und der Dyson-Schwinger-Gleichung auf, die das GW-Modell erfüllt. Daraus folgen weiters interessante Zusammenhänge zwischen (2n-2) und 2n-Punkt- Korrelationsfunktionen die in einem späteren Abschnitt für den speziellen Fall des Zusammenhangs von 2- und 4-Punkt-Funktion wiederum explizit berechnet werden. Im letzten Teil dieser Arbeit werden die Techniken des allgemeinen Beweises auf das Langmann-Szabo-Zarembo-Modell angewandt. Dies ist ein GW-Modell im äußeren Magnetfeld und stellt damit auch ein interessantes Testmodell für ein besseres Verständnis des Quanten-Hall-Effektes dar.

Bibliography

[1] Shiraz Minwalla, Mark Van Raamsdonk, and Nathan Seiberg. Noncommutative perturbative dynamics. *JHEP*, 0002:020, 2000.

[2] Edwin Langmann and Richard J. Szabo. Duality in scalar field theory on noncommutative phase spaces. *Phys. Lett.*, B533:168–177, 2002.

[3] Harald Grosse and Raimar Wulkenhaar. Power-counting theorem for non-local matrix models and renormalisation. *Commun. Math. Phys.*, 254:91–127, 2005.

[4] Harald Grosse and Raimar Wulkenhaar. Renormalisation of ϕ^4 theory on noncommutative $\mathbb{R}^2$ in the matrix base. *JHEP*, 12:019, 2003.

[5] Harald Grosse and Raimar Wulkenhaar. Renormalisation of ϕ^4 theory on noncommutative $\mathbb{R}^4$ in the matrix base. *Commun. Math. Phys.*, 256:305–374, 2005.

[6] Harald Grosse and Harold Steinacker. Renormalization of the noncommutative ϕ^3 model through the kontsevich model. *Nuclear Physics B*, 746:202, 2006.

[7] Fabien Vignes-Tourneret. Renormalization of the orientable non-commutative gross-neveu model, 2007.

[8] Harald Grosse and Raimar Wulkenhaar. The beta-function in duality-covariant noncommutative ϕ^4 theory. *Eur. Phys. J.*, C35:277–282, 2004.

[9] Margherita Disertori and Vincent Rivasseau. Two and three loops beta function of non commutative ϕ^4_4 theory. *European Physical Journal C*, 50:661, 2007.

[10] M. Disertori, R. Gurau, J. Magnen, and V. Rivasseau. Vanishing of beta function of non commutative ϕ^4_4 theory to all orders. *Physics Letters B*, 649:95, 2007.

[11] Vincent Rivasseau. Non-commutative renormalization, 2007.

[12] John Collins. *Renormalization*. Cambridge Monographs, 1995.

[13] Joseph Ben Geloun, Razvan Gurau, and Vincent Rivasseau. Vanishing beta function for grosse-wulkenhaar model in a magnetic field. *Physics Letters B*, 671:284, 2009.

[14] L.C.Q. Vilar, O.S. Ventura, D.G. Tedesco, and V.E.R. Lemes. Renormalizable noncommutative u(1) gauge theory without ir/uv mixing. *arXiv: hep-th/0902.2956*, 2009. hep-th/0902.2956.

Thomas Kaltenbrunner

Staudingergasse 14/18
1200 Vienna
Austria

✉ *tkaltenbrunner@gmail.com*

Personal Details

• Nationality:	Austria
• Birthplace:	Vienna, Austria
• Date of birth:	16.08.1982
• Address	Staudingergasse 14/18, 1200 Vienna, Austria

Education

- **Study of Mathematical Physics**
  since October 2003, anticipated graduation date: April 2008
  University of Vienna, Austria
  Title of Tesis: Noncommutative QFT at the Self-Dual Point
- **Secondary Education**

1996 - 2001	Handelsakademie Gänserndorf (HAK) Gänserndorf, Austria
1992 - 1996	Real-Gymnasium Gänserndorf Gänserndorf, Austria

- **Elementary School**
  1988 - 1992 VS Strasshof, Strasshof, Austria

Stay abroad

- **Universidad de Santiago de Chile, Chile**
  July 2006 - December 2006 Joint Study Programme

Work History

- Miscellaneous minor employments 2001 - 2009
  at OMV, Vienna Intl. Airport, Central Library of Physics

Other Activities

- Civilian Service at the Red Cross, Gänserndorf 2001

Science Interests

- QFT, Noncommutative Geometry, Matrix Models, Renormalization Group, Phase Transitions

Additional Skills

- **Languages**
  German (mother tongue)
  English
  Spanish
- **Computer Skills**
  Mathematica
  Latex
  Programming Language "C" (basic skills)
  MS Office

Vienna, März 2008